Two-field screening and its cosmological dynamics

Philippe Brax[1,2] and Ayoub Ouazzani[1,3]
[1]*Institut de Physique Théorique, Université Paris-Saclay, CEA, CNRS, F-91191 Gif-sur-Yvette Cedex, France*
[2]*CERN, Theoretical Physics Department, CH 1211 Geneva 23, Switzerland*
[3]*Département de Physique de l'Ecole Normale Supérieure, F-75230 Paris, France*

(Received 1 August 2023; accepted 25 August 2023; published 18 September 2023)

We consider the screening of the axio-dilaton fields when both the dilaton and the axion couple to matter with Yukawa couplings. We analyze the screening of the dilaton in the vicinity of a compact object and find that this can only take place when special boundary conditions at infinity are imposed. We study the cosmological dynamics of the axio-dilaton system when linearly coupled to matter and find that the special boundary conditions at infinity, which guarantee the screening of compact objects, do not generically emerge from cosmology. We analyze the background cosmology and the cosmological perturbations at late times in these models and show that the baryon acoustic oscillations constrain the coupling of the dilaton to matter to be smaller than in its natural supergravity realization. Moreover, we find that the Hubble rate in the present Universe could deviate from the normalized Planck value, although by an amount too small to account for the H_0 tension, and that the growth of the structure is generically reduced compared to ΛCDM.

DOI: 10.1103/PhysRevD.108.063517

I. INTRODUCTION

General relativity (GR) effectively passes all the current gravitational tests in the solar system [1]. Yet there is still tension on larger scales, which may eventually necessitate challenging Einstein's theory of gravity. These are related to two classes of observations. First, there are long-standing astrophysical results that imply the existence of dark matter [2]. Second, there is now robust evidence in favor of the acceleration of the expansion of the Universe [3,4]. The latter is best accounted for in GR by adding a cosmological constant to the Lagrangian of the theory. However, understanding the origin of this constant energy density, e.g., from quantum field theoretic considerations, has proven to be fraught with difficulties [5]. Modifying GR is not an easy task either [6]. We know from Lovelock's theorem [7] and, in the effective field theory context, from Weinberg's theorem [8] that GR is unique in four dimensions provided Lorentz invariance and the masslessness of the graviton hold [9].

One way to modify GR is to add additional fields. This is the route taken by scalar-tensor theories [10] in which one or more additional scalar fields are added to the setting and couple to matter. Such scalar fields appear in many proposed dynamical models attempting to account for the late cosmic acceleration [11]. They also find theoretical motivation in the fact that they appear naturally in UV-complete theories such as string theory [12,13]. In particular, the swampland conjectures favor an explanation of the late-time acceleration of the Universe resulting from the nontrivial dynamics of string moduli [14]. We present the axio-dilaton, which is one such scalar-tensor theory whose origin can be traced to a compactification of ten to four dimensions [13].

Unfortunately, most scalar-tensor theories are typically ruled out by solar system tests of gravity. In their most naive form, consistency of scalar-tensor theories either requires them to have a small coupling to matter or the scalar must be stabilized with large masses leading to short-ranged interactions [15].

This can be illustrated with the Brans-Dicke theory (BD) and the action [1,16]

$$\mathcal{S}_{\rm BD} = \int d^4x\sqrt{-g}M_p^2\left(\frac{\mathcal{R}}{2} - \frac{1}{2}\partial^\mu\varphi\partial_\mu\varphi - V(\varphi)\right) + \mathcal{S}_m(g^J_{\mu\nu}, \psi_m) \tag{1}$$

where ψ_m represents the ordinary matter fields and the Jordan frame metric is given by

$$g^J_{\mu\nu} = A^2(\varphi)g_{\mu\nu} \quad \text{with} \quad A(\varphi) = e^{\mathfrak{g}\varphi} \tag{2}$$

where $\mathfrak{g}$ is a coupling constant. The scalar couples to matter only via the metric $g^J_{\mu_\nu}$. The metric $g_{\mu\nu}$ is the Einstein metric

for which the Einstein equations take their usual form; i.e., matter "feels" the geometry of the Jordan frame.

Constraints from solar system tests like those using measurements by the Cassini probe [17] can be understood using the parametrized post-Newtonian (PPN) formalism. It is enough here to define two important PPN parameters. We introduce the gravitational mass of the source M, and the PPN parameters $\gamma_{\rm PPN}$, $\beta_{\rm PPN}$ via the following parametrization of the Jordan metric element in isotropic coordinates around a given compact object,

$$ds_J^2 = -\left(1 - \frac{2GM}{r} + 2\beta_{\rm PPN}\left(\frac{GM}{r}\right)^2 + \mathcal{O}\left(\frac{1}{r^3}\right)\right)dt^2 + \left(1 + 2\gamma_{\rm PPN}\frac{GM}{r} + \mathcal{O}\left(\frac{1}{r^2}\right)\right)(dr^2 + r^2 d\Omega^2). \quad (3)$$

In GR $\gamma_{\rm PPN} = \beta_{\rm PPN} = 1$ while for the Brans-Dicke theory the deviation from GR is captured by $\gamma_{\rm PPN}$, i.e., $\beta_{\rm PPN} = 1$ and [13]

$$\gamma_{\rm PPN} = \frac{1 - 2\mathfrak{g}^2}{1 + 2\mathfrak{g}^2}. \quad (4)$$

The Cassini probe, on the other hand, gives [17]

$$|\gamma_{\rm PPN} - 1| < 2.3 \times 10^{-5}. \quad (5)$$

This constrains the coupling $\mathfrak{g}^2$ to be less than 10^{-5}.

Larger deviations from GR can be reached in certain regimes when the theories are subject to a screening mechanism, i.e., a modification which allows the theory to evade solar system tests while having an order unity coupling to matter whose role is important on large scales. There are now at least three types of screening mechanisms for single field models, i.e., the chameleon, K-mouflage, and Vainshtein mechanisms [18–20]. They all rely on higher derivatives and/or nonlinearities of the kinetic terms and interacting potentials of the models [15]. In [13], a new screening mechanism was introduced, which relies on a second field that has a nonzero but small coupling to matter. The mechanism depends crucially on the interplay between the scalar profiles inside and outside matter [21,22]. Here, we consider the situations where the two fields, the dilaton and the axion, have a linear coupling to matter, which we denote by κ and ϵ. We focus on the small ϵ regime and vary κ from small values up to unity, which corresponds to its value in supergravity where the dilaton plays the role of the volume modulus of string compactifications [23]. We find that for $\kappa = 1$, screening of the dilaton around compact objects only takes place when the fields take particular values at infinity. These values should emerge from the cosmological dynamics. We then focus on the cosmology of these values where both κ and the values of the coupling ϵ to both baryons and cold dark matter are varied. Generically, the field values in the present Universe do not satisfy the screening conditions. In fact, one must resort to yet unknown screening mechanisms for the axio-dilaton system in order to accommodate both local solar system tests and cosmological constraints such as the baryon acoustic oscillations [24].

The coupling of the axion to dark matter ϵ_C plays a crucial role cosmologically and can be of order unity. On the other hand, we find that the coupling of the dilation κ must be reduced locally to small values in order to pass solar system tests. In this paper, we consider two likely scenarios. The first one is that the coupling κ is determined locally to be extremely small, of the order of 10^{-3}, and that most of the cosmological dynamics are due to the coupling of the axion ϵ_C in a manner reminiscent of coupled quintessence [25], although in a multifield setting here [26]. This could be achieved if another field χ drove the coupling κ to such values dynamically in the whole Universe. Another possibility could be that the coupling κ is small locally but allowed to take larger values cosmologically. This could happen if the field χ only made κ small locally. In this second scenario, we find that the baryon acoustic oscillation (BAO) constraints on late time cosmology are so stringent that κ cannot be taken of order unity as in the original supergravity model. In this setting, we consider the allowed deviations of H_0 from their values as calibrated by the Planck satellite experiment and find that only a few percent of discrepancy is allowed. This is much less than the current H_0 tension [27,28]. Finally, we notice that the linear growth in these models is reduced compared to the ΛCDM case, despite the existence of attractive fifth forces due to the dilaton and the axion. This could provide a solution to the σ_8 tension [29] where the observed amount of clustering is reduced compared to the expected one from early times [30,31]. The precise study of this possibility is left to future work.

The scenario that we present here enlarges the usual single-field class of models for late time cosmology. Such multifield generalizations could prove useful in view of future measurements and present cosmological tensions [32].

The paper is arranged as follows. In Sec. II, we present the axio-dilaton model. In Sec. III, we consider the screening of compact objects. We then discuss the cosmology of these models in Sec. IV.

II. AXIO-DILATON THEORY

A. Lagrangian

The axio-dilaton theory contains two scalar fields, the dilaton $\tau > 0$ and the axion a. The dilaton τ couples to matter only through the Jordan frame metric while a is directly coupled to matter. The difference is made clear below where we construct an effective metric which mediates the coupling of both scalars to matter. The action of the theory is

$$\mathcal{S}=\int d^4x\sqrt{-g}M_p^2\left[\frac{\mathcal{R}}{2}-\frac{3}{4}\left(\frac{\partial^\mu\tau\partial_\mu\tau+\partial^\mu a\partial_\mu a}{\tau^2}\right)\right]+\mathcal{S}_m, \tag{6}$$

with

$$\mathcal{S}_m=\mathcal{S}_m(g^J_{\mu\nu},a,\psi_m),\qquad g^J_{\mu_\nu}=A(\tau)^2g_{\mu\nu},$$
$$A(\tau)=\tau^{-\kappa/2}. \tag{7}$$

Here, κ is a coupling constant. The theory studied in [13] corresponds to $\kappa=1$ and is associated to a supergravity model of string theory origin with a Kähler potential $K=-3\ln(\mathcal{T}+\bar{\mathcal{T}})$ and a coupling to matter determined by $A=e^{K/6}$. In this setting, the dilaton can be seen as the volume modulus of a 6D compatification of string theory from 10D to 4D. Introducing κ enables one to tune the matter-dilaton coupling and make the solar system tests of gravity easier to satisfy. We see that screening is compulsory for the model to pass the solar system tests of gravitation.

The two fields can be viewed as the real and imaginary parts of a complex field $\mathcal{T}=\frac{1}{2}(\tau+ia)$ whose Lagrangian is

$$\mathcal{L}=\sqrt{-g}M_p^2\left(\frac{\mathcal{R}}{2}-\frac{3\partial^\mu\mathcal{T}\partial_\mu\bar{\mathcal{T}}}{(\mathcal{T}+\bar{\mathcal{T}})^2}\right)+\mathcal{L}_m. \tag{8}$$

In this model, we define the usual stress-energy tensor and the coupling of a to matter,

$$T^{\mu\nu}\equiv-\frac{2}{\sqrt{-g}}\frac{\delta S_m}{\delta g_{\mu\nu}},\qquad \mathcal{A}\equiv-\frac{2}{\sqrt{-g}}\frac{\delta S_m}{\delta a}. \tag{9}$$

For the trace, we use the notation $T\equiv g_{\mu\nu}T^{\mu\nu}$. Notice that the matter action depends on the axion field in a nontrivial manner and not via the Jordan metric. This has drastic consequences, which we unravel below.

There are two Klein-Gordon equations for the two scalar fields, i.e.,

$$\Box\tau-\frac{1}{\tau}(\partial_\mu\tau\partial^\mu\tau-\partial_\mu a\partial^\mu a)-\kappa\frac{\tau}{3M_p^2}T=0 \tag{10}$$

and

$$\Box a-\frac{2}{\tau}\partial_\mu\tau\partial^\mu a+\frac{\tau^2}{3M_p^2}\mathcal{A}=0. \tag{11}$$

It is convenient to introduce the dilaton field φ such that $\tau=e^\varphi$, leading to

$$\Box\varphi+(\partial_\mu a\partial^\mu a)e^{-2\varphi}-\frac{\kappa}{3M_p^2}T=0. \tag{12}$$

The Einstein equation is simply

$$\mathcal{R}_{\mu\nu}-\frac{3}{2\tau^2}(\partial_\mu\tau\partial_\nu\tau+\partial_\mu a\partial_\nu a)-\frac{1}{M_p^2}\left(T_{\mu\nu}-\frac{1}{2}Tg_{\mu\nu}\right)=0. \tag{13}$$

where we have separated the matter energy-momentum tensor from the scalar one.

B. Symmetries

In the absence of matter, the theory is invariant under a $SL(2,\mathbb{R})$ group whose origin can be traced back to supergravity. Indeed, the kinetic term of the fields is invariant under

$$\mathcal{T}\to\frac{a\mathcal{T}-ib}{ic\mathcal{T}+d}\qquad\text{provided}\qquad ad-bd=1 \tag{14}$$

corresponding to a Kähler transformation of the theory. There are thus three conserved currents, corresponding to the dimension of the symmetry group in the absence of matter. As a basis for these currents, we can choose the following:

(i) The axion shift symmetry $\mathcal{T}\to\mathcal{T}-ib$ ($a=c=0$, $d=1$):

$$J^\mu_A=\frac{\partial^\mu a}{\tau^2}. \tag{15}$$

(ii) The rescaling symmetry $\mathcal{T}\to a\mathcal{T}$ ($b=c=0$, $d=1$):

$$J^\mu_S=\frac{\partial^\mu\tau}{\tau}+\frac{a\partial^\mu a}{\tau^2}. \tag{16}$$

(iii) The nonlinear symmetry $\mathcal{T}\to\mathcal{T}-ic\mathcal{T}^2$ ($a=d=1$, $b=0$, $c\ll1$):

$$J^\mu_N=\frac{\tau^2-a^2}{\tau^2}\partial^\mu a-2a\frac{\partial^\mu\tau}{\tau}. \tag{17}$$

From the Klein-Gordon equations we can directly obtain the (non)conservation laws

$$\nabla_\mu J^\mu_A=-\frac{\mathcal{A}}{3M_p^2},\qquad \nabla_\mu J^\mu_S=\frac{\kappa T-a\mathcal{A}}{3M_p^2},$$
$$\nabla_\mu J^\mu_N=\frac{(a^2-\tau^2)\mathcal{A}-2a\kappa T}{3M_p^2}. \tag{18}$$

As can be seen, matter breaks the whole symmetry group as none of the three currents is conserved anymore.

When $\mathcal{S}_m$ does not depend on a, i.e., $\mathcal{A}=0$, the axio-dilation theory is equivalent to a Brans-Dicke theory. Indeed, when $\mathcal{A}=0$ we have the axion solution $a=$ cste, so Eq. (12) becomes

$$\Box\varphi - \frac{\kappa}{3M_p^2}T = 0. \tag{19}$$

Similarly, the BD Lagrangian (50) gives the Klein-Gordon equation

$$\Box\varphi_{\rm BD} + \frac{\mathfrak{g}}{M_p^2}T = 0. \tag{20}$$

Matching the two Weyl factors $e^{-\kappa\varphi/2} = e^{\mathfrak{g}\varphi_{\rm BD}}$, we get $\varphi_{\rm BD} = (-\kappa/2\mathfrak{g})\varphi$. Combining the two Klein-Gordon equations

$$\left(\frac{-\kappa}{2\mathfrak{g}} + \frac{3\mathfrak{g}}{\kappa}\right)\Box\varphi = 0 \Rightarrow \mathfrak{g}^2 = \kappa^2/6. \tag{21}$$

When $\kappa = 1$, we find that the coupling reduces to $1/\sqrt{6}$, i.e., the same as for $f(R)$ and massive gravity.

III. NONRELATIVISTIC SOURCE AND SCREENING

Screening requires one to study the gravitational physics around objects like the Sun. We model the Sun and other compact objects such as the Earth or the Moon as nonrelativistic sources; i.e., the only nonzero component of their stress-energy tensor is $T_{00} \equiv \rho$. We also assume that they are static and spherically symmetric. We look for space-time solutions with the same symmetries, which we chart with isotropic coordinates,

$$g_{\mu\nu}dx^\mu dx^\nu = -e^{2u(r)}dt^2 + e^{2w(r)}(dr^2 + r^2d\Omega^2). \tag{22}$$

The Jordan metric is obtained by multiplying this line element by the coupling function A^2.

A. Exterior solution

We simplify the setting by considering nonrelativistic objects with a small Newtonian potential. As a result, we approximate the Klein-Gordon equations using a flat background $\boldsymbol{g} = \boldsymbol{\eta}$, where $\eta_{\mu\nu}$ is the Minkowski metric tensor. The validity of the approximation is evaluated *a posteriori*.

In the following, primes refer to derivatives with respect to r. We assume spherical symmetry. The resulting Klein-Gordon equations are

$$\tau'' + \frac{2\tau'}{r} - \frac{\tau'^2 - a'^2}{\tau} + \kappa\frac{\tau\rho}{3M_p^2} = 0 \tag{23}$$

and

$$a'' + \frac{2a'}{r} - \frac{2\tau' a'}{\tau} + \frac{\tau^2\mathcal{A}}{3M_p^2} = 0. \tag{24}$$

Here ρ is the matter density inside or outside the object. Instead of using these equations directly, we can use the equations for the currents (18). In the absence of matter, i.e., outside the objects, the currents are conserved:

$$r^2\frac{a'}{\tau^2} = C_A, \tag{25}$$

$$r^2\left(\frac{\tau'}{\tau} + \frac{aa'}{\tau^2}\right) = C_S, \tag{26}$$

$$r^2\left(\frac{(\tau^2 - a^2)a'}{\tau^2} - \frac{2a\tau'}{\tau}\right) = C_N. \tag{27}$$

These constants are fixed by the conditions inside the source.

We are interested in the case where $a \neq$ cste. Thus, $C_A \neq 0$. Defining $\gamma \equiv C_A$, $\alpha \equiv C_S/C_A$, $\beta \equiv (C_S/C_A)^2 + C_N/C_A$, we obtain

$$\tau^2 + (a - \alpha)^2 = \beta^2, \tag{28}$$

where τ and a thus evolve on a circle in the $\tau - a$ plane. Therefore, we can eliminate τ in Eq. (25) and obtain

$$a' = \frac{\gamma}{r^2}(\beta^2 - (a - \alpha)^2). \tag{29}$$

We integrate this to obtain the axion profile

$$a = \alpha - \beta\tanh X(r) \quad \text{with} \quad X(r) = \frac{\gamma\beta}{r} + \delta, \tag{30}$$

where δ is a new integration constant. Using Eq. (25) again, we finally obtain

$$\tau = \frac{\beta}{\cosh X(r)}. \tag{31}$$

Some of the integration constants are fixed by the boundary conditions inside the source. Indeed, from the currents (18), we see that

$$\gamma = C_A = -\frac{1}{3M_p^2}\int_0^R drr^2\mathcal{A}(r), \tag{32}$$

$$\gamma\alpha = C_S = -\frac{1}{3M_p^2}\int_0^R drr^2(\kappa\rho(r) + a(r)\mathcal{A}(r)). \tag{33}$$

On the other hand, β and δ can only be fixed by the values of the fields at infinity,

$$a_\infty = \alpha - \beta\tanh\delta, \qquad \beta = \tau_\infty\cosh\delta = \sqrt{\tau_\infty^2 + (\alpha - a_\infty)^2}. \tag{34}$$

As shown in the Appendix, these solutions in the flat background approximation are valid as long as

$$r \gg GM \quad \text{and} \quad r \gg |\gamma\beta|. \tag{35}$$

The first condition corresponds to being far from the Schwarzschild radius.

B. Screening

We first investigate screening in the Jordan frame where we extract the PPN parameters from the Jordan metric,

$$\begin{aligned} g^J_{\mu\nu}dx^\mu dx^\nu &= A^2 g_{\mu\nu}dx^\mu dx^\nu \\ &= -\left(1-\frac{2GM_g}{r}+2\beta_{\rm PPN}\left(\frac{GM_g}{r}\right)^2+\mathcal{O}\left(\frac{1}{r^3}\right)\right)dt^2 \\ &\quad +\left(1+2\gamma_{\rm PPN}\frac{GM_g}{r}+\mathcal{O}\left(\frac{1}{r^2}\right)\right)(dr^2+r^2d\Omega^2), \end{aligned} \tag{36}$$

where $A^2 = 1/\tau^\kappa$ and $g_{\mu\nu}$ is given by (22). Here, M_g is the gravitational mass as defined in the PPN formalism. We have that $M_g \neq M = \int_{\rm source}\rho$; i.e., the mass of the object in the Jordan frame is renormalized by the presence of the scalar fields.

In the absence of fields, the Einstein frame metric $g_{\mu\nu}$ is the Schwarzschild metric. In the presence of the fields, the Einstein equations are modified, and we expand as

$$e^{2u} = 1-\frac{2l}{r}+\frac{2l^2}{r^2}+\mathcal{O}\left(\frac{1}{r^3}\right), \tag{37}$$

$$e^{2w} = 1+\frac{2l}{r}+\mathcal{O}\left(\frac{1}{r^3}\right), \tag{38}$$

where $l = GM$. Expanding the conformal factor A^2 in inverse powers of the distance, we have

$$A^2 = A^2_\infty\left(1-\alpha_1/r+\alpha_2/r^2+\mathcal{O}\left(\frac{1}{r^3}\right)\right), \tag{39}$$

from which we deduce that

$$\gamma_{\rm PPN} = \frac{1-\frac{\alpha_1}{2l}}{1+\frac{\alpha_1}{2l}}, \tag{40}$$

$$\beta_{\rm PPN} = \frac{l^2+l\alpha_1+\frac{1}{2}\alpha_2}{(l+\frac{1}{2}\alpha_1)^2}. \tag{41}$$

For the axio-dilaton theory the conformal factor is given by

$$A^2 = \tau^{-\kappa} = \left(\frac{\cosh(\frac{\beta\gamma}{r}+\delta)}{\beta}\right)^\kappa \tag{42}$$

where we have used the explicit solution for $\tau(r)$. Expanding in $1/r$ we find the coefficients

$$\begin{aligned} \alpha_1 &= -\kappa\beta\gamma\tanh\delta, \\ \alpha_2 &= \frac{\kappa\beta^2\gamma^2}{2}((\kappa-1)\tanh^2\delta+1). \end{aligned} \tag{43}$$

In the following, we always choose the ansatz [13]

$$\mathcal{A} = -\epsilon T, \tag{44}$$

where ϵ is a small constant and T the trace of the energy-momentum tensor. In the case of static sources this reduces to $\mathcal{A} = \epsilon\rho$. As we see, this choice is not innocent as it brings back the two-field model within the realm of the scalar-tensor theories with an effective coupling to both the dilaton and the axion. We make this explicit in the following. From Eq. (32) we obtain

$$\gamma = -\frac{2\epsilon GM}{3} = -\frac{2\epsilon l}{3}, \tag{45}$$

and in the Jordan frame the PPN parameters become

$$\gamma_{\rm PPN} = \frac{3-\epsilon\kappa\beta\tanh\delta}{3+\epsilon\kappa\beta\tanh\delta} \tag{46}$$

and

$$\beta_{\rm PPN} = 1+\frac{\kappa\epsilon^2\beta^2(1-\tanh^2\delta)}{(3+\kappa\epsilon\beta\tanh\delta)^2}.$$

Hence, by taking ϵ small, GR is recovered as long as β does not increase accordingly. This is the essence of this new type of screening, which corresponds to a nonuniform limit $\epsilon \to 0$. Indeed, when $\epsilon = 0$ the model is equivalent to a Brans-Dicke model with a coupling $\kappa/\sqrt{6}$ which needs to be small enough to satisfy the solar system tests of gravity. However, it turns out that the nonuniform limit $\epsilon \to 0$ requires particular boundary conditions at infinity which are not generic. We come back to this point in the next section.

C. Interior solution

We now solve Eqs. (23) and (24) inside the source of radius R, with the boundary conditions $\tau'(0) = a'(0) = 0$ at the origin. We assume a uniform density inside the body as a simplifying assumption and a coupling $\mathcal{A}$ with the same profile as ρ,

$$\begin{cases} \rho \equiv \rho_0 = \frac{M}{\frac{4}{3}\pi R^3} \\ \mathcal{A} = \epsilon\rho_0. \end{cases} \tag{47}$$

The dynamical equations cannot be solved exactly. We obtain perturbative solutions in ϵ as we have seen that a small coupling ϵ is required to screen in the Jordan frame.

1. Dilaton dynamics

The equation for the current J^μ_A from Eq. (18) gives

$$\left(r^2\frac{a'}{\tau^2}\right)' = -\frac{r^2\mathcal{A}}{3M_p^2}. \tag{48}$$

Assuming regularity for the fields at the origin, we obtain

$$\frac{a'(r)}{\tau^2(r)} = -\frac{\epsilon\rho_0}{3M_p^2 r^2}\frac{r^3}{3}. \tag{49}$$

We define $m^2 = \rho_0/3M_p^2$, leading to

$$a' = -\frac{\epsilon m^2}{3} r\tau^2. \tag{50}$$

We can substitute this expression in Eq. (23) to get

$$\tau'' + \frac{2\tau'}{r} - \frac{(\tau')^2}{\tau} + \frac{\epsilon^2 m^4}{9} r^2\tau^3 + \kappa m^2\tau = 0. \tag{51}$$

In terms of the dilaton $\varphi = \ln\tau$, the Klein-Gordon equation (12) then becomes

$$\varphi'' + \frac{2}{r}\varphi' + \frac{\epsilon^2 m^4}{9} r^2 e^{2\varphi} + \kappa m^2 = 0 \tag{52}$$

where we impose the boundary equation $\varphi'(0) = 0$.

2. Perturbative expansion in ϵ

Up to now, everything is exact. We now expand in powers of ϵ:

$$\varphi = \varphi^{(0)} + \epsilon\varphi^{(1)} + \ldots, \tag{53}$$

$$a = a^{(0)} + \epsilon a^{(1)} + \ldots, \tag{54}$$

and impose the boundary conditions at each order.

The advantage of this perturbative method is that the problematic term $e^{2\varphi}$ in Eq. (52) appears only at second order in ϵ. Indeed, at orders 0 and 1, we obtain

$$\varphi^{(0)\prime\prime} + \frac{2}{r}\varphi^{(0)\prime} + \kappa m^2 = 0, \tag{55}$$

$$\varphi^{(1)\prime\prime} + \frac{2}{r}\varphi^{(1)\prime} = 0. \tag{56}$$

The solution for $\varphi^{(1)}$ is then

$$\varphi^{(1)} = c_0 + \frac{c_1}{r}. \tag{57}$$

For $\varphi^{(0)}$ we have

$$\varphi^{(0)} = d_0 + \frac{d_1}{r} - \frac{\kappa m^2}{6} r^2. \tag{58}$$

The boundary conditions $\varphi^{(n)\prime}(0) = 0$ impose that the fields are regular at 0, so we have no $1/r$ term, i.e., $c_1 = d_1 = 0$, and finally

$$\tau = (\tau_0 + \epsilon\tau_1) e^{-\frac{\kappa m^2}{6} r^2} + \ldots \tag{59}$$

where we have redefined the constants of integration. Inside the source and for small ϵ, τ decreases exponentially fast.

We can now obtain a. Using Eq. (50) we have

$$a^{(0)\prime} + \epsilon a^{(1)\prime} = \epsilon\frac{\tau_0^2}{2}(e^{-\frac{\kappa m^2}{3} r^2})', \tag{60}$$

and therefore

$$a^{(0)} = \text{cste}, \tag{61}$$

$$a^{(1)} = \frac{\tau_0^2}{2} e^{-\frac{\kappa m^2}{3} r^2} + \text{cste}. \tag{62}$$

The axion field is then given by

$$a = a_0 + \epsilon\left(a_1 + \frac{\tau_0^2}{2} e^{-\frac{\kappa m^2}{3} r^2}\right) + \ldots. \tag{63}$$

We see that the axion and dilaton fields only evolve when $\epsilon \neq 0$.

3. Matching to the exterior solution

The continuity of τ and a at $r = R$ reads

$$(\tau_0 + \epsilon\tau_1) e^{-\frac{\kappa m^2}{6} R^2} = \frac{\beta}{\cosh(\frac{\beta\gamma}{R} + \delta)}, \tag{64}$$

$$a_0 + \epsilon\left(a_1 + \frac{\tau_0^2}{2} e^{-\frac{\kappa m^2}{3} R^2}\right) = \alpha - \beta\tanh\left(\frac{\beta\gamma}{R} + \delta\right). \tag{65}$$

We use the continuity equations for $\varphi' = \tau'/\tau$ and a'/τ^2,

$$-\frac{\kappa m^2}{3} R = \tanh\left(\frac{\beta\gamma}{R} + \delta\right)\frac{\beta\gamma}{R^2}, \tag{66}$$

$$-\frac{\epsilon\kappa\tau_0^2 m^2}{3(\tau_0 + \epsilon\tau_1)^2} R = \frac{\gamma}{R^2}. \tag{67}$$

Thus, we have eight integration constants, i.e., $\alpha, \beta, \gamma, \delta$ for the exterior solution and τ_0, τ_1, a_0, a_1 for the interior solution. Recall that

$$\gamma = -\frac{\epsilon m^2}{3} R^3, \tag{68}$$

$$\gamma\alpha = -m^2 \int_0^R dr r^2(\kappa + \epsilon a(r)). \tag{69}$$

Thus, γ is fixed independently of the others, and α depends on a_0 and a_1. We are left with six parameters. With a system of four continuity constraints as given above, we end up with 2 degrees of freedom. These can be parametrized by the values of the fields at infinity τ_∞ and a_∞ which determine the full solution.

D. Screening revisited

We can now revisit the conditions under which the gravitational deviation from GR in the Jordan frame is small. Using

$$\gamma\alpha = -\frac{1}{3M_p^2} \int_0^R dr r^2(\kappa\rho(r) + a(r)\mathcal{A}(r)) \tag{70}$$

and $\gamma = -\epsilon m^2 R^3/3$, we obtain the identity

$$\frac{-\epsilon m^2 R^3}{3}\alpha = -m^2\left(\kappa\frac{R^3}{3} + \epsilon\int_0^R dr r^2 a^{(0)}(r) + \epsilon^2\int_0^R dr r^2 a^{(1)}(r)\right). \tag{71}$$

As a result, the expansion of α is singular in the limit $\epsilon \ll 1$ and becomes

$$\alpha = \frac{\kappa}{\epsilon} + a_0 + \epsilon a_1 + \ldots, \tag{72}$$

implying that the outside solution is very sensitive to small values of ϵ. In particular, we see that the limit of small $\epsilon \ll 1$ leads to a large value for the exterior axion field. Using Eq. (34) we obtain

$$\beta = \sqrt{\tau_\infty^2 + \left(\frac{\kappa}{\epsilon} + a_0 - a_\infty^{(0)}\right)^2} \tag{73}$$

where we have neglected the terms of order ϵ. Now, unless a_∞ turns out to be of order $1/\epsilon$ and cancels exactly the term in κ/ϵ, we find that for generic boundary values at infinity

$$\beta = \frac{\kappa}{\epsilon} + a_0 - a_\infty^{(0)} + \ldots \tag{74}$$

when $\kappa = \mathcal{O}(1)$ and $\epsilon \ll 1$. The matching conditions at $r = R$ simplify as we notice that $m^2R^2/2 = G_N M/R$, where M is the mass of the object. This is nothing but the Newtonian potential of the compact object at its surface which is always small in our Newtonian approximation, its value being close to 10^{-6} for the Sun. We then deduce, using (65), that $a_0 = a_\infty^{(0)}$ to leading order, and similarly

$$\tanh\delta = 1 - \frac{\epsilon^2}{\kappa}\frac{\tau_0^2}{2} + \ldots, \tag{75}$$

implying that δ is always large. As a result we have $\epsilon\beta\tanh\delta = \kappa + \cdots$, and the PPN parameters are simply the ones of a scalar tensor theory with a coupling $\kappa/\sqrt{6}$,

$$\gamma_{\rm PPN} = \frac{3-\kappa^2}{3+\kappa^2} + \mathcal{O}(\epsilon) \tag{76}$$

and

$$\beta_{\rm PPN} = 1 + \mathcal{O}(\epsilon^2). \tag{77}$$

In this limit $\beta_{\rm PPN}$ can be arbitrarily close to 1 for small ϵ, but not $\gamma_{\rm PPN}$. Small deviations of $\gamma_{\rm PPN}$ from unity are only achieved for very small κ, a result which does not differ from Brans-Dicke's, signaling that screening does not take place. Screening can only take place when

$$a_\infty^{(0)} - a_0 = \frac{\kappa}{\epsilon}, \tag{78}$$

which corresponds to a specific choice for the axion field at infinity. As the theory has no scalar potential, the value of the axion field at infinity is not obtained by minimizing an effective potential like in the chameleon mechanism. Hence, the boundary value of the axion field must emerge from the cosmological dynamics. We study this below.

Our analysis has assumed that $\mathcal{A} = \epsilon\rho$. As soon as the dependence of the matter action on the axion is weak, i.e., $\mathcal{A}/\rho \sim \epsilon \ll 1$, the same qualitative results follow as γ will be of order ϵ and $\gamma\alpha$ of order κ. This reasoning is independent of the details of the model inside the source.

E. Effective metric

As we have seen, the generic absence of screening leads to the coupling of a compact object to be equivalent to the one of a point particle with coupling $\kappa/\sqrt{6}$. This is the coupling of matter to the dilaton. The fact that the axion couples to the matter action, too, implies that compact objects do not follow the geodesics of the Jordan metric but the ones of an effective metric whose presence can be inferred from the small field expansion

$$\delta S_m = -\int d^4x\sqrt{-g}\left(\frac{\partial \ln A}{\partial\varphi}\delta\varphi - \frac{\epsilon}{2}\delta a\right)T \tag{79}$$

where the variation of the fields is taken around the background values for the dilaton and the axion. Notice that the axion and the dilaton fields both couple to the trace of the energy-momentum tensor. Let us define

$$B(\varphi, a) = A(\varphi)e^{-\epsilon a/2}. \tag{80}$$

Then the coupling to matter can be written as

$$\delta S_m = -\int d^4x\sqrt{-g}\left(\frac{\partial \ln B}{\partial \varphi}\delta\varphi + \frac{\partial \ln B}{\partial a}\delta a\right)T \tag{81}$$

corresponding to the coupling of a two-field scalar-tensor theory where the effective metric is

$$g^{\rm eff}_{\mu\nu} = B^2(\varphi, a)g_{\mu\nu}. \tag{82}$$

As a result, compact objects evolve along the geodesics of the effective metric and not the Jordan metric.

This can be confirmed by analyzing the geodesic equations for pressureless matter for the axio-dilaton theories. Indeed, the Klein-Gordon equations and the Bianchi identity $\nabla^\mu(R_{\mu\nu} - \frac{R}{2}g_{\mu\nu}) = 0$ imply the nonconservation equation

$$\nabla_\mu T^{\mu\nu} = \frac{1}{2}(\kappa T\partial^\nu\varphi - \mathcal{A}\partial^\nu a). \tag{83}$$

For nonrelativistic matter, the energy-momentum tensor is simply

$$T_{\mu\nu} = \rho u_\mu u_\nu \quad \text{with} \quad u_\mu u^\mu = -1. \tag{84}$$

In this section, dots denote the time derivative along the particle lines defined by u^μ, i.e., $\dot{X} \equiv \nabla_u X = u^\mu\nabla_\mu X$. For scalar quantities X, this also corresponds to the derivative with respect to the proper time of a particle moving with velocity u^μ. We define the local Hubble rate as $3h \equiv \nabla_\mu u^\mu$. The nonconservation equation then becomes

$$\dot{\rho}u^\mu + 3h\rho u^\mu = \frac{1}{2}(\kappa\rho\partial^\mu\varphi + \mathcal{A}\partial^\mu a). \tag{85}$$

Contracting with u_μ and using $u^\mu u_\mu = -1$ we get the generalized continuity equation

$$\dot{\rho} + 3h\rho = -\frac{1}{2}(\kappa\rho\dot{\varphi} + \mathcal{A}\dot{a}). \tag{86}$$

We recognize the coupling function B,

$$B \equiv e^{-\frac{1}{2}(\kappa\varphi + \epsilon a)}, \tag{87}$$

when $\epsilon = $ cste. We can define a conserved density $\rho_{\rm con}$ in the Einstein frame such that

$$\rho = B\rho_{\rm con} \tag{88}$$

as

$$\dot{\rho}_{\rm con} + 3h\rho_{\rm con} = 0. \tag{89}$$

This is the conserved matter density in the axio-dilaton setting. Combining Eqs. (85) and (86), we obtain the modified Newton law

$$\dot{u}^\mu - \frac{1}{2}(\kappa\dot{\varphi} + \epsilon\dot{a})u^\mu = \frac{1}{2}(\kappa\partial^\mu\varphi + \epsilon\partial^\mu a). \tag{90}$$

This reads

$$\dot{u}^\mu + \frac{d\ln B}{d\eta}u^\mu = -\partial^\mu \ln B, \tag{91}$$

where η is the proper time. With m_0 defining the mass of the particles, we find that the effective mass of these particles in the Einstein frame is dressed by the scalar field and becomes

$$m = B(\varphi, a)m_0. \tag{92}$$

This follows from the identification $\rho = m\delta^{(4)}(x^\mu - x^\mu(\tau))$ along the particle's trajectory and $\rho_{\rm con} = m_0\delta^{(4)}(x^\mu - x^\mu(\tau))$. The momentum of each particle becomes

$$p^\mu = mu^\mu. \tag{93}$$

Newton's law then becomes

$$\dot{p}^\mu = -m\partial^\mu \ln B. \tag{94}$$

As a result, a force deriving from the potential $\ln B$ is exerted on each particle whose mass is also field dependent. For instance, in the nonrelativistic limit and in the presence of gravity, Newton's law becomes

$$\frac{dp^i}{dt} = -m\partial^i\Phi \tag{95}$$

where Φ_N is Newton's potential and

$$\Phi = \Phi_N + \ln B \tag{96}$$

combines the effects of gravity and the scalar field. This modification of Newton's law is nothing but the one which can be derived from the coupling of matter to the effective metric $g^{\rm eff}_{\mu\nu}$. As a result, we have confirmed that compact objects do not follow the geodesics of the Jordan metric but rather the one of the effective metric. We analyze the cosmological consequences of this result below.

F. Effective charge

Let us come back to the effective scalar charge carried by a compact object. We have seen that in the $\epsilon \ll 1$ limit and unless the fields at infinity take special values, which should be adjusted cosmologically, the objects are not screened. Far away from a given object we expect the acceleration of another object due to the scalar field to fall off as

$$a^i \simeq -\frac{2Q^2 G_N M}{r^3} r^i \tag{97}$$

where Q is the scalar charge of both objects. Here M is the mass of the object responsible for the acceleration of the second body. The charges of both objects are equal as no screening takes place. Using

$$\ln B = -\frac{1}{2}(\kappa\varphi + \epsilon a) \supset \frac{1}{2}(\kappa \ln\ \cosh X(r) + \epsilon\beta \tanh X(r)) \tag{98}$$

and identifying this as $-2Q^2 G_N M/r$ at large distances, we find that far away from the object

$$2Q^2 G_N M = -\frac{\gamma\beta}{2}(\kappa \tanh\delta + \epsilon\beta(1 - \tanh^2\delta)) \tag{99}$$

and for $\epsilon \ll 1$ we retrieve

$$Q = \frac{\kappa}{\sqrt{6}} \tag{100}$$

up to corrections of order ϵ^2. The resulting interaction including gravity is equivalent to rescaling Newton's constant as

$$G_{\text{eff}} = (1 + 2Q^2) G_N \tag{101}$$

with $\Phi = -G_{\text{eff}} M/r$. As expected in this limit corresponding to $\epsilon \ll \kappa$, the coupling of the axion field to matter becomes negligible for far-away objects, and the coupling is the same as in the Jordan frame.

In conclusion, we find that $\kappa \lesssim 10^{-3}$ for the Cassini test to be evaded. This is a very small value which could only be avoided if the cosmological values of the axion and dilaton fields were tuned cosmologically.

G. Numerical integration

In this section, we find numerical solutions of the equations around a massive sphere.

1. Setting the numerical problem

The Klein-Gordon equations with the constant source inside a ball of radius R have the form

$$\tau'' + \frac{2\tau'}{r} - \frac{(\tau')^2}{\tau} + \frac{(a')^2}{\tau} + \frac{\kappa\rho_0\tau}{3M_p^2}\theta(r) = 0, \tag{102}$$

$$a'' + \frac{2a'}{r} - \frac{2a'\tau'}{\tau} + \frac{\epsilon\rho_0\tau^2}{3M_p^2}\theta(r) = 0, \tag{103}$$

where $\theta(r)$ is the step function that goes from 1 to 0 at the radius of the source R. We introduce the characteristic length $L = \sqrt{3M_p^2/\rho_0} = m^{-1}$ and write $r = \hat{r}L$. We obtain the dimensionless equations

$$\tau'' + \frac{2\tau'}{\hat{r}} - \frac{(\tau')^2}{\tau} + \frac{(a')^2}{\tau} + \kappa\theta(\hat{r})\tau = 0, \tag{104}$$

$$a'' + \frac{2a'}{\hat{r}} - \frac{2a'\tau'}{\tau} + \epsilon\theta(\hat{r})\tau^2 = 0, \tag{105}$$

which we solve with the initial conditions $\tau'(0) = a'(0) = 0$. We also regularize the step function, e.g., $\hat{\theta}(\hat{r}) = \frac{1}{2}(\tanh(N\frac{\hat{R}-\hat{r}}{\hat{R}}) + 1)$, to have a transition of width $\sim\hat{R}/N$. Notice that $\hat{R} = R/L = \sqrt{2GM/R}$, i.e., the square root of the ratio of the Schwarzschild radius to the radius of the source. For the Sun, $\hat{R}_\odot = 2.05 \times 10^{-3}$.

2. Results

We see in the example in Fig. 1 that we obtain a perfect match with the exterior solution but also with the first order interior solution. The variations of the fields are relatively small, i.e., of order 10^{-6} relative to the value at the center. For other sets of parameters the variation increases with the initial value at the center and of course the values of κ and ϵ.

The equations that we have used in the flat metric approximation are valid only for

$$r \gg GM, \qquad r \gg |\gamma\beta|. \tag{106}$$

With $R = \hat{R}L$, we have

$$r \gg GM \Leftrightarrow \hat{r} \gg \frac{\hat{R}^3}{2}. \tag{107}$$

For the Sun, $\hat{R}_\odot^3 \sim 10^{-8}$. One can trust our description of the static solution apart from a small region around the origin. Similarly, we have $\gamma = -\epsilon\hat{R}^3 L/3$, so we obtain

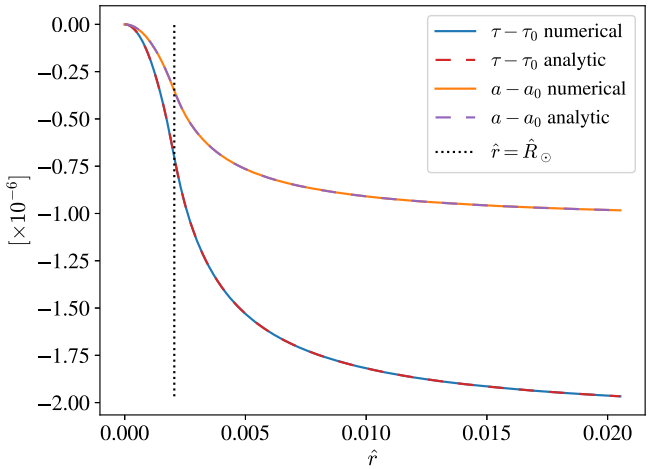

FIG. 1. Field profiles for $\hat{R} = \hat{R}_\odot$, $\kappa = 1$, and $\epsilon = 0.5$. The initial values are taken such that $\tau_0 = a_0 = 1$, $\tau'(0) = a'(0) = 0$.

$$r \gg |\gamma\beta| \Leftrightarrow \hat{r} \gg \hat{R}^3 \frac{\epsilon\beta}{3}, \tag{108}$$

which excludes a very small region around the origin.

IV. AXIO-DILATON COSMOLOGY

A. Two-fluid model

In the following, we concentrate on models where two fluids are present, i.e., the baryons and cold dark matter (CDM) with couplings determined by κ to the dilaton and $\epsilon_{B,C}$ to the axion. We have seen that κ and ϵ_B, i.e., the coupling of the baryons to the axion, must be small to comply with the solar system tests unless the fields take special values at infinity. This translates into a choice of boundary conditions for the fields on cosmological scales. We see that this situation is not generic and that, starting from initial conditions in the radiation era which do not perturb the background cosmology, the cosmological dynamics do not drive the fields to special values now.

The energy-momentum tensor of matter is taken to be

$$T^{B,C}_{\mu\nu} = \rho_{B,C} u^{B,C}_\mu u^{B,C}_\nu \tag{109}$$

corresponding to the baryons B and CDM C. We also assume here, for definiteness,

$$\mathcal{A} = -\epsilon_C T_C - \epsilon_B T_B \tag{110}$$

where $T_{B,C} = -\rho_{B,C}$ are the baryonic and CDM densities, respectively. The matter energy-momentum tensors are not conserved but satisfy the nonconservation equations

$$\nabla_\mu T^{\mu\nu}_i = \frac{1}{2}(\kappa T_i \partial^\nu \varphi + \epsilon_i T_i \partial^\nu a) \tag{111}$$

where $i = B,\ C$. This implies that the total energy-momentum tensor

$$T^{\mu\nu} = T^{\mu\nu}_B + T^{\mu\nu}_C \tag{112}$$

satisfies the nonconservation equation

$$\nabla_\mu T^{\mu\nu} = \frac{1}{2}(\kappa T \partial^\nu \varphi - \mathcal{A}\partial^\nu a) \tag{113}$$

which is a consequence of the Bianchi identity.

In this section, we denote the time derivative along the particle lines, defined by u^μ_i, by $d/d\tau_i = u^\mu_i \nabla_\mu$ We define the local Hubble rate as $3h_i \equiv \nabla_\mu u^\mu_i$. Notice that the covariant derivatives are calculated in the Einstein frame; hence, this is the local Hubble rate along the particle lines as measured using the geometry of the Einstein frame. The nonconservation equations for each species then become

$$\frac{d\rho_i}{d\tau_i} + 3h_i\rho_i = -\frac{1}{2}(\kappa\dot{\varphi} + \epsilon_i \dot{a})\rho_i. \tag{114}$$

We define the coupling function B_i as

$$B_i \equiv e^{-\frac{1}{2}(\kappa\varphi + \epsilon_i a)} \tag{115}$$

when $\epsilon_i = \text{cste}$. We can now introduce a conserved density $\rho_{\text{con,i}}$ in the Einstein frame such that

$$\rho_i = B_i \rho_{\text{con,i}} \tag{116}$$

and

$$\frac{d\rho_{\text{con},i}}{d\tau_i} + 3h_i\rho_{\text{con,i}} = 0. \tag{117}$$

This is the conserved matter density in the axio-dilaton setting. Similarly, we obtain the modified Newton law

$$\frac{du^\mu_i}{d\tau_i} + \frac{d\chi_i}{d\tau_i} u^\mu_i = -\partial^\mu \chi_i \tag{118}$$

where

$$\chi_i \equiv \ln B_i. \tag{119}$$

For each species, we can define an effective metric

$$g^i_{\mu\nu} = B_i^2 g_{\mu\nu} \tag{120}$$

which corresponds to the Jordan frame for the given species. As $B_B \neq B_C$, we see that the Jordan frames for CDM and the baryons do not coincide.

We apply this formalism first to the background cosmological case and then to the cosmological perturbations.

B. Spatially flat cosmology

We are interested in the cosmology of a homogeneous and isotropic universe in the presence of the axio-dilaton fields. The FLRW (Friedmann-Lemaître-Robertson-Walker) metric reads

$$\begin{aligned} g_{\mu\nu}dx^\mu dx^\nu &= -dt^2 + R^2(t)\gamma_{ij}dx^i dx^j \\ &= -dt^2 + R^2(t)\left(\frac{dr^2}{1-kr^2} + r^2 d\Omega^2\right) \end{aligned} \tag{121}$$

where R is the scale factor. We define, as usual, the Hubble rate as $H = \dot{R}/R$. In the following we focus on the spatially flat case $k = 0$.

We assume that the fields are irrelevant in the early Universe up until some redshift z_i which will typically be the matter-radiation equality. Indeed, in the radiation era the matter density is negligible, and therefore the fields are hardly influenced by their matter couplings. As a result they

remain constant if their initial velocities vanish. This also guarantees that the influence of the axio-dilaton system on big bang nucleosynthesis (BBN) is minimal. We choose the initial conditions for the fields φ, a, and their derivatives such that they vanish at z_i. This does not correspond to the values of the fields for which screening takes place. On the other hand, this entails a vanishing energy density for the axion and dilatons initially.

Each species has its own Jordan frame with the background metric

$$g^i_{\mu\nu}dx^\mu dx^\nu = -dt_i^2 + R_i^2 dx^i dx_i \tag{122}$$

where the cosmic time and the scale factor are defined by

$$dt_i = B_i dt, \qquad R_i = B_i R. \tag{123}$$

As CDM is not subject to the precision tests in the solar system, we allow for large values of ϵ_C. Moreover, we consider the effects on the scale factor in the Jordan frame of the baryons $R_B = B_B R$ corresponding to the conservation of baryonic matter. We use the convention that $R_B = 1$ today and identify the redshift as detected from transition lines of atoms by

$$1 + z = R_B^{-1}. \tag{124}$$

Although we focus on the dynamics in the baryon frame, we first study the equations of motion in the Einstein frame.

C. Klein-Gordon equations

We look for time-dependent solutions for the scalar fields $\tau(t)$ and $a(t)$ of the Klein-Gordon equations

$$\ddot{\tau} + 3H\dot{\tau} - \frac{\dot{\tau}^2 - \dot{a}^2}{\tau} - \frac{\kappa\tau\rho}{3M_p^2} = 0 \tag{125}$$

and

$$\ddot{a} + 3H\dot{a} - \frac{2\dot{\tau}\,\dot{a}}{\tau} - \frac{\tau^2\mathcal{A}}{3M_p^2} = 0. \tag{126}$$

Here the total matter density is $\rho = \rho_B + \rho_C$ and $\mathcal{A} = \epsilon_B\rho_B + \epsilon_C\rho_C$. Notice that these equations are valid both in the radiation and matter eras. In the radiation era, the source terms depend on the matter density only as the trace of the radiation energy-momentum tensor vanishes. As a first approximation, we neglect the source terms in the radiation era. This implies that $\dot{a} \approx 0$ and $\dot{\phi} \approx 0$, and the field hardly moves during the radiation era. In our numerical analysis, we are interested in the physics in the matter era, and we fix the initial conditions at matter-radiation equality. A detailed analysis of the model from the end of inflation through radiation to the matter era is left for future work. We consider that the fields start evolving significantly when the matter era begins.

D. Continuity equations

The energy density and pressure carried by the two scalar fields are given by

$$\rho_f = \frac{3M_p^2}{4}\left(\frac{\dot{\tau}^2 + \dot{a}^2}{\tau^2}\right) \tag{127}$$

and

$$p_f = \frac{3M_p^2}{4}\left(\frac{\dot{\tau}^2 + \dot{a}^2}{\tau^2}\right), \tag{128}$$

corresponding to a perfect fluid with equation of state $\omega_f = 1$. Using the Bianchi identity and the Einstein equation in the Einstein frame, we obtain that the total energy is conserved, i.e.,

$$\dot{\rho} + \dot{\rho}_f + 3H(\rho + \rho_f + P + P_f) = 0, \tag{129}$$

where the pressure terms have been included. This leads to

$$\dot{\rho} + \dot{\rho}_f + 3H(\rho + 2\rho_f) = 0. \tag{130}$$

Using the identity

$$\dot{\rho}_f = \frac{3M_p^2}{4}\frac{2}{\tau^3}(\tau\dot{\tau}\,\ddot{\tau} + \tau\dot{a}\,\ddot{a} - \dot{\tau}^3 - \dot{\tau}\dot{a}^2) \tag{131}$$

and the expression of $\ddot{\tau}$ and $\ddot{a}$ in the Klein-Gordon equations, Eqs. (125) and (126), we obtain

$$\dot{\rho}_f + 6H\rho_f = \frac{1}{2}\left(\kappa\rho\frac{\dot{\tau}}{\tau} + \mathcal{A}\dot{a}\right). \tag{132}$$

Finally, using the continuity equation we obtain

$$\dot{\rho} + 3H\rho + \frac{1}{2}(\kappa\rho\dot{\varphi} + \mathcal{A}\dot{a}) = 0 \tag{133}$$

as we have argued previously. This is associated with the nonconservation equations per species,

$$\dot{\rho}_i + 3H\rho_i + \frac{1}{2}\rho_i(\kappa\dot{\varphi} + \epsilon_i\dot{a}) = 0. \tag{134}$$

This can be integrated exactly and leads to

$$\rho = \rho_B + \rho_C = B_B\frac{\rho_{0B}}{R^3} + B_C\frac{\rho_{0C}}{R^3}. \tag{135}$$

Notice that if we define

$$\rho = B\frac{\rho_0}{R^3} \tag{136}$$

then $B = \lambda_B B_B + \lambda_C B_C$ where the fraction of baryons and CDM is $\lambda_i = \frac{\rho_{0i}}{\rho_0}$ where $\rho_0 = \rho_{0B} + \rho_{0C}$. In practice, we have $\lambda_B = \frac{\Omega_{0B}}{\Omega_{0B}+\Omega_{0C}}$ where $\Omega_{0B} \simeq 0.022$ and $\Omega_{0C} \simeq 0.12$ from the Planck experiment [3]. Here and in the following, we normalize the density ρ_0 to the Planck value as deduced from early-time physics compared to the late-time effects on the matter density that we study below.

E. Friedmann equations

The Friedmann equation is obtained from the (00) component of the Einstein equation and becomes

$$H^2 = \frac{\rho}{3M_p^2} + \frac{\rho_f}{3M_p^2} + \frac{\rho_\Lambda}{3M_p^2}, \tag{137}$$

where we have introduced a cosmological constant associated with the energy density ρ_Λ. The Raychaudhuri equation from the (*ii*) Einstein equation reads

$$\frac{\ddot{R}}{R} = -\frac{1}{6M_p^2}(\rho + \rho_f + \rho_\Lambda + 3(P + P_f + P_\Lambda)), \tag{138}$$

leading to

$$\frac{\ddot{R}}{R} = -\frac{1}{6M_p^2}(\rho + 4\rho_f - 2\rho_\Lambda). \tag{139}$$

These equations are defined in the Einstein frame and will be transformed into the effective frame for baryons below.

We thus have the following system of differential equations for R, τ, and a only:

$$\begin{aligned} &\ddot{\tau} + 3H\dot{\tau} - \frac{\dot{\tau}^2 - \dot{a}^2}{\tau} - \kappa\frac{\rho(\tau,a)}{3M_p^2}\tau = 0,\\ &\ddot{a} + 3H\dot{a} - \frac{2\dot{\tau}\,\dot{a}}{\tau} - \epsilon\frac{\rho(\tau,a)}{3M_p^2}\tau^2 = 0,\\ &\dot{R} = H(\tau,a)R, \end{aligned} \tag{140}$$

with the Friedmann equations

$$\begin{aligned} &H^2 = \frac{\rho}{3M_p^2} + \frac{\rho_f}{3M_p^2} + \frac{\rho_\Lambda}{3M_p^2},\\ &\rho = B_B\frac{\rho_{0B}}{R^3} + B_C\frac{\rho_{0C}}{R^3}, \qquad \rho_f = \frac{3M_p^2}{4}\left(\frac{\dot{\tau}^2 + \dot{a}^2}{\tau^2}\right),\\ &\frac{d\ln B_i}{dt} = -\frac{1}{2}(\kappa\dot{\varphi} + \epsilon_i\dot{a}). \end{aligned} \tag{141}$$

We solve these equations numerically for different values of ϵ and κ.

F. Dynamics in the effective baryon frame

In the baryon frame, the Hubble rate is

$$H_B \equiv \frac{d\ln R_B}{dt_B} = \frac{H}{B_B} + \frac{d\chi_B}{dt_B}. \tag{142}$$

The conserved baryon density in the baryon frame is simply

$$\tilde{\rho}_B \equiv \rho_{\mathrm{con}B} = \frac{\rho_{0B}}{R_B^3}. \tag{143}$$

In this frame, CDM is not conserved, but an observer fitting the evolution of the Universe with a prior that CDM is also conserved in the same frame as the baryons would identify the conserved CDM density as

$$\tilde{\rho}_C = \frac{\rho_{0C}}{R_B^3}, \tag{144}$$

and we could write an effective Friedmann equation in the baryonic frame,

$$H_B^2 \equiv \frac{8\pi G_B}{3}\tilde{\rho}_B + \frac{8\pi G_C}{3}\tilde{\rho}_C + \frac{8\pi G_N}{3}\tilde{\rho}_\Lambda, \tag{145}$$

where we have used $8\pi G_N = 1/M_{\mathrm{p}}^2$. This allows one to identify the effective Newton constants $G_{B,C}$ and the dark energy component $\overline{\rho}_\Lambda$. None of these constants is constant in the baryon frame. In practice, the effective Newton constants are determined by

$$G_B = B_B^2 G_N, \qquad G_C = B_B B_C G_N; \tag{146}$$

i.e., the two Newtonian constants evolve differently. The dark energy component is simply defined as the complement to the baryon and CDM contributions in the baryonic Friedmann equation.

As long as the fields do not evolve rapidly, i.e., at the beginning of the matter era, we have $H_B \approx H/B_B$. The dark energy component becomes

$$\tilde{\rho}_\Lambda = \frac{\rho_f + \rho_\Lambda}{B_B^2}. \tag{147}$$

In the late Universe, this identification is not valid anymore, and a numerical integration of the equations of motion is necessary.

The same Friedmann equation in the baryon frame can be written as

$$\Omega_B^B + \Omega_C^B + \Omega_\Lambda^B = 1 \tag{148}$$

where the energy fractions Ω_i^B, $i = B, C, \Lambda$ are identified in the baryon frame and are such that

$$\Omega^B_{B,C} = \frac{8\pi G_{B,C}\tilde{\rho}_{B,C}}{3H_B^2}, \qquad \Omega^B_{\Lambda} = \frac{8\pi G_N \tilde{\rho}_{\Lambda}}{3H_B^2}. \tag{149}$$

The deviations of the energy fractions from ΛCDM are represented in Fig. 5.

G. Deviations from ΛCDM and observational constraints

We first define the effective gravitational constant that an observation would measure. For example, big bang nucleosynthesis (BBN) puts constraints on the variation of such a $G_{\rm eff}$ [33,34]:

$$|\Delta G/G| \equiv \left| \frac{G_{\rm eff}^{\rm today} - G_{\rm eff}^{\rm BBN}}{G_{\rm eff}^{\rm BBN}} \right| < 0.4. \tag{150}$$

This assumes a Hubble evolution similar to that of ΛCDM in the matter-dominated era. In our model, since observations are made in the baryon frame, the corresponding $G_{\rm eff}$ satisfies

$$H_B^2 = \frac{8\pi}{3} G_{\rm eff}\left[\frac{c_\rho}{R_B^3} + \rho_{\Lambda,B}\right], \tag{151}$$

for some c_ρ. In order to have $G_{\rm eff}(z_i) = G_N$ initially, we set $c_\rho = \rho_0$, as defined by Eq. (136); i.e., we normalize Newton's constant by using the Planck normalization in the early Universe. Since the physics between BBN and $z = z_i$ is the same as in the standard model, $G_{\rm eff} = G_N$ until $z = z_i$. Later, the relative variation of the effective coupling to baryons can be computed between $z = z_i$ and today:

$$\left.\frac{\Delta G_B}{G_B}\right|_{\rm BBN\to today} = \left.\frac{\Delta G_B}{G_B}\right|_{z_i\to \rm today}. \tag{152}$$

We can further constrain the possible deviations of the Hubble rate from the standard model by imposing that this should be less than the discrepancy appearing in the H_0 tension. Indeed, there are two diverging determinations of the present-time Hubble rate H_0 with a relative difference of order 10% [28]. In the axio-dilaton theory, the fact that Newton's constant varies implies that the Hubble rate now differs from the corresponding Hubble rate in the standard model. We have normalized the Hubble rates to coincide at the beginning of the matter era. This motivates us to look for parameters that satisfy

$$\left|\frac{\Delta H_B}{H_B}\right|_{\rm tension} \equiv \left|\frac{H_B(z=0) - H_{\rm SM}(z=0)}{H_{\rm SM}(z=0)}\right| < 0.1, \tag{153}$$

where $H_{\rm SM}$ is the Hubble rate in the standard model. Another stringent constraint comes from BAO [24] which specify that the deviations of $H_B(z)$ for $0.2 \lesssim z \lesssim 2.5$ should be less than around 3% [24],

$$\left|\frac{\Delta H_B}{H_B}\right|_{\rm BAO} \equiv \left|\frac{H_B(z\in[0.2,2.5]) - H_B^{\rm SM}(z\in[0.2,2.5])}{H_B^{\rm SM}(z\in[0.2,2.5])}\right| < 0.03. \tag{154}$$

This implies that the differences between Λ-CDM and the axio-dilaton models must appear late in the evolution of the Universe. We see that the BAO constraint is the most stringent one amongst the ones we have selected. Of course, a much more precise numerical study is required to constrain the parameter space. This is left to future work.

We also consider the effective equation of state of dark energy. In GR with matter, in addition to a fluid X with equation of state w, the deceleration parameter

$$q_0 := -\left|\frac{\ddot{R}}{RH^2}\right|_{\rm today} \tag{155}$$

is given by

$$q_0 = \frac{1}{2}(\Omega_{m,0} + (1+3\omega)\Omega_{X,0}) \tag{156}$$

where $\Omega_{i,0} = \rho_i(z=0)/3M_p^2H_0^2$. Observations thus give an estimate for w depending on $\Omega_{m,0}$. For $\Omega_{m,0} \sim 0.3$, which can be obtained independently, this leads to [35,36]

$$w \sim -1 \pm 0.1. \tag{157}$$

Recent constraints and future prospects can be found in [37]. We now define the effective equation of state

$$w_{\rm eff} \equiv \frac{1}{3}\frac{2q_{B,0} - \Omega_{m,0}}{\Omega_{\Lambda,0}} - 1, \tag{158}$$

where

$$q_{B,0} = -\left.\frac{\partial^2_{t_B} R_B}{R_B H_B^2}\right|_{\rm today}. \tag{159}$$

Taking $\Omega_{m,0} \simeq 0.3$, we must impose the constraint

$$|\Delta w| \equiv |w_{\rm eff} + 1| \lesssim 0.1. \tag{160}$$

We use this bound in what follows as a guiding principle. We are not trying to give a precise fit to the data but an indication on the parameter space compatible with cosmology.

H. Numerical integration

1. Dimensionless equations

In the following, we use $L = \sqrt{3M_P^2/\rho_0}$ as the unit of time and length. Here ρ_0 is defined via Eq. (135). We obtain quantities as functions of redshift starting at

matter-radiation equality. We define the system of dynamical equations with the number of e-folds N and φ such that $R = e^N$ and $\tau = e^{\varphi}$. We obtain

$$\ddot{\varphi} = -3\hat{H}\,\dot{\varphi} - \dot{a}^2 e^{-2\varphi} + \kappa\hat{\rho},$$
$$\ddot{a} = -3\hat{H}\,\dot{a} + 2\dot{\varphi}\,\dot{a} + \epsilon\hat{\rho}e^{2\varphi},$$
$$\dot{N} = \hat{H},$$

with

$$\hat{H}^2 = \hat{\rho} + \hat{\rho}_f + \hat{\rho}_\Lambda, \qquad \hat{\rho} = Be^{-3N},$$
$$\hat{\rho}_f = \frac{1}{4}(\dot{\varphi}^2 + \dot{a}^2 e^{-2\varphi}). \tag{161}$$

Here $\hat{\rho}_\Lambda$ corresponds to ρ_Λ/ρ_0 where ρ_Λ is the density associated with the cosmological constant. In ΛCDM, ρ_0 is also the value of the matter density today, so $\hat{\rho}_\Lambda = \Omega_{\Lambda,0}/\Omega_{m,0} \simeq 7/3$ in ΛCDM. It is convenient to work in conformal time η, such that $Rd\eta = dt$, implying that

$$\varphi'' = -2\hat{\mathcal{H}}\varphi' - a'^2 e^{-2\varphi} + \kappa\tilde{\rho},$$
$$a'' = -2\hat{\mathcal{H}}a' + 2\varphi' a' + \epsilon\tilde{\rho}e^{2\varphi},$$
$$N' = \hat{\mathcal{H}}, \tag{162}$$

with

$$\hat{\mathcal{H}}^2 = \check{\rho} + \check{\rho}_f + \check{\rho}_\Lambda, \tag{163}$$

where the derivatives are now with respect to η. We have rescaled all the densities as $\check{\rho} = e^{2N}\hat{\rho}$ and similarly for the scalar and dark energy parts.

2. Results

There are four main parameters: κ, ϵ_B, ϵ_C, and $\hat{\rho}_\Lambda$. Following our discussion about screening in Sec. III D and our identification of the effective metric in Sec. IV A, we first take κ and ϵ_B to be small. Taking $\kappa = \epsilon_B = 10^{-3}$ turns out to be enough to satisfy solar system constraints. Taking one of them to be 1 order of magnitude higher leads to a violation of the cosmological constraints when ϵ_C is large

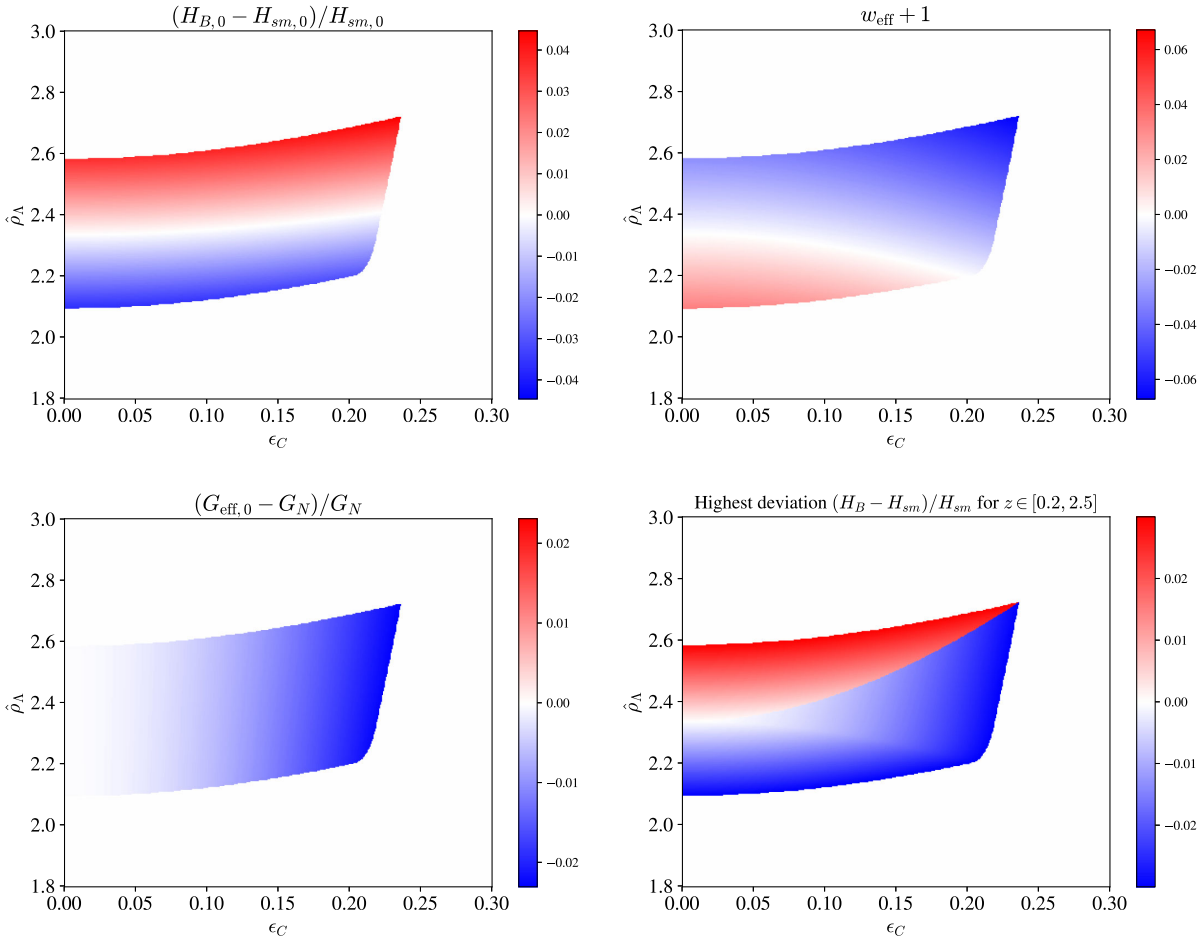

FIG. 2. Values of the parameters which satisfy the cosmological tests for $\kappa = 10^{-3}$ and $\epsilon_B = 10^{-3}$. Note that 602×602 points are plotted. The colored regions satisfy the four constraints $|\Delta H_0/H_0| < 0.1$, $|\Delta w| < 0.1$, $|\Delta G/G| < 0.4$, $|\Delta H/H|_{\rm BAO} < 0.03$.

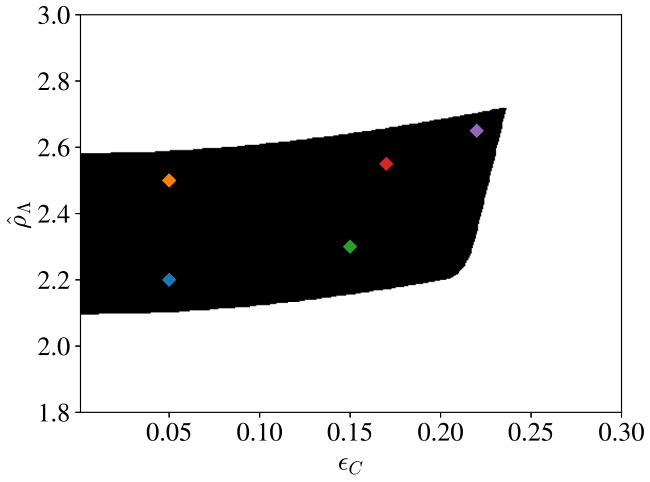

FIG. 3. Positions of a selection of parameters in the region of parameter space where the cosmological tests are satisfied: $\epsilon_C = 0.05, \hat{\rho}_\Lambda = 2.2$; $\epsilon_C = 0.05, \hat{\rho}_\Lambda = 2.5$; $\epsilon_C = 0.15, \hat{\rho}_\Lambda = 2.3$; $\epsilon_C = 0.17, \hat{\rho}_\Lambda = 2.55$; $\epsilon_C = 0.22, \hat{\rho}_\Lambda = 2.65$.

enough. Numerically we study the cosmological evolution for a large range of values of ϵ_C and $\hat{\rho}_\Lambda$. We always start the cosmological evolution at $z_i = 3400 \approx z_{\rm eq}$.

A first picture of the deviations from ΛCDM can be obtained by focusing on the cosmological tests (Newton's constant, the equation of state, the Hubble parameter today and in $z \in [0.2, 2.5]$ relative to that of the standard model) we defined above and their consequences as viewed in the $\epsilon - \hat{\rho}_\Lambda$ plane. This is shown in Fig. 2. We show their values only for the region in which the four of them satisfy the observational constraints. It turns out that the constraint from BAO is always the strongest. We illustrate the cosmological evolution using five sets of parameters in Figs. 4–6. Standard model quantities are computed analytically from the ΛCDM solutions in the matter-dominated era with $\Omega_{\Lambda,0}/\Omega_{m,0} = 7/3$.

We recover that the smallest deviations to ΛCDM are for $\epsilon_C = 0, \hat{\rho}_\Lambda \simeq 7/3$. We observe that deviations of H_0 depend mostly on $\hat{\rho}_\Lambda$ while deviations of G are essentially given by ϵ_C. Additionally, we see deviations which are both positive and negative for H_0, with the sign depending on the sign of the deviation of $\hat{\rho}_\Lambda$ compared to $\approx 7/3$. On the other hand, there are only negative deviations of G. As we observe in Fig. 4, ϵa increases, so G_B decreases.

For both H_0 and $w_{\rm eff}$, the deviations due to ϵ_C tend to be compensated by deviations of $\hat{\rho}_\Lambda$. This can be understood from the fact that the fields act as a fluid of equation of state $w_f = 1$ opposite to that of the cosmological constant $w_\Lambda = -1$. They have opposite effects on the cosmic acceleration.

Moving on to the dynamical curves, we see in Fig. 4 the evolution of the fields. The axion a increases with z, which can be expected as the source term in its Klein-Gordon equation (126) has a factor $\epsilon > 0$ and initially dominates. On the other hand, φ slightly increases at first but eventually decreases much more. This can be expected, as the source term in its Klein-Gordon equation has a factor $\kappa > 0$ which initially dominates, and later the source term is dominated by the axion term proportional to $-\dot{a}^2$. The deviation from the constant and vanishing fields increases with ϵ as we can expect.

Figure 5 shows the evolution of the energy content of the Universe in both the Einstein and baryon frames. As the couplings κ and ϵ_B are small, the difference between the Einstein and the baryon frame quantities is negligible. In the matter-dominated era we have a slight increase in the field density and a corresponding decrease of the matter density. In the very late Universe close to a vanishing redshift, the proportion of the cosmological constant increases, and we get the usual values 0.3 and 0.7 for matter and Λ with some deviations of the order of 0.01.

As a result, we can see that, generically, the matter contents of the Universe are modified. First of all, the axion and dilaton energy densities evolve from being negligible

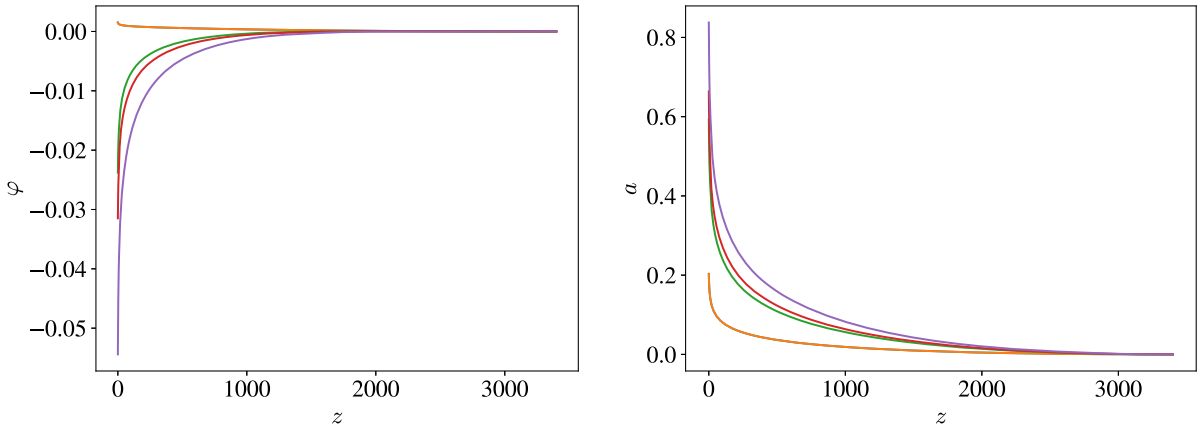

FIG. 4. Field evolutions for $\kappa = 10^{-3}$ and $\epsilon_B = 10^{-3}$ as a function of the redshift z defined in the baryon frame. The values of ϵ_C and $\hat{\rho}_\Lambda$ for each color are given in Fig. 3.

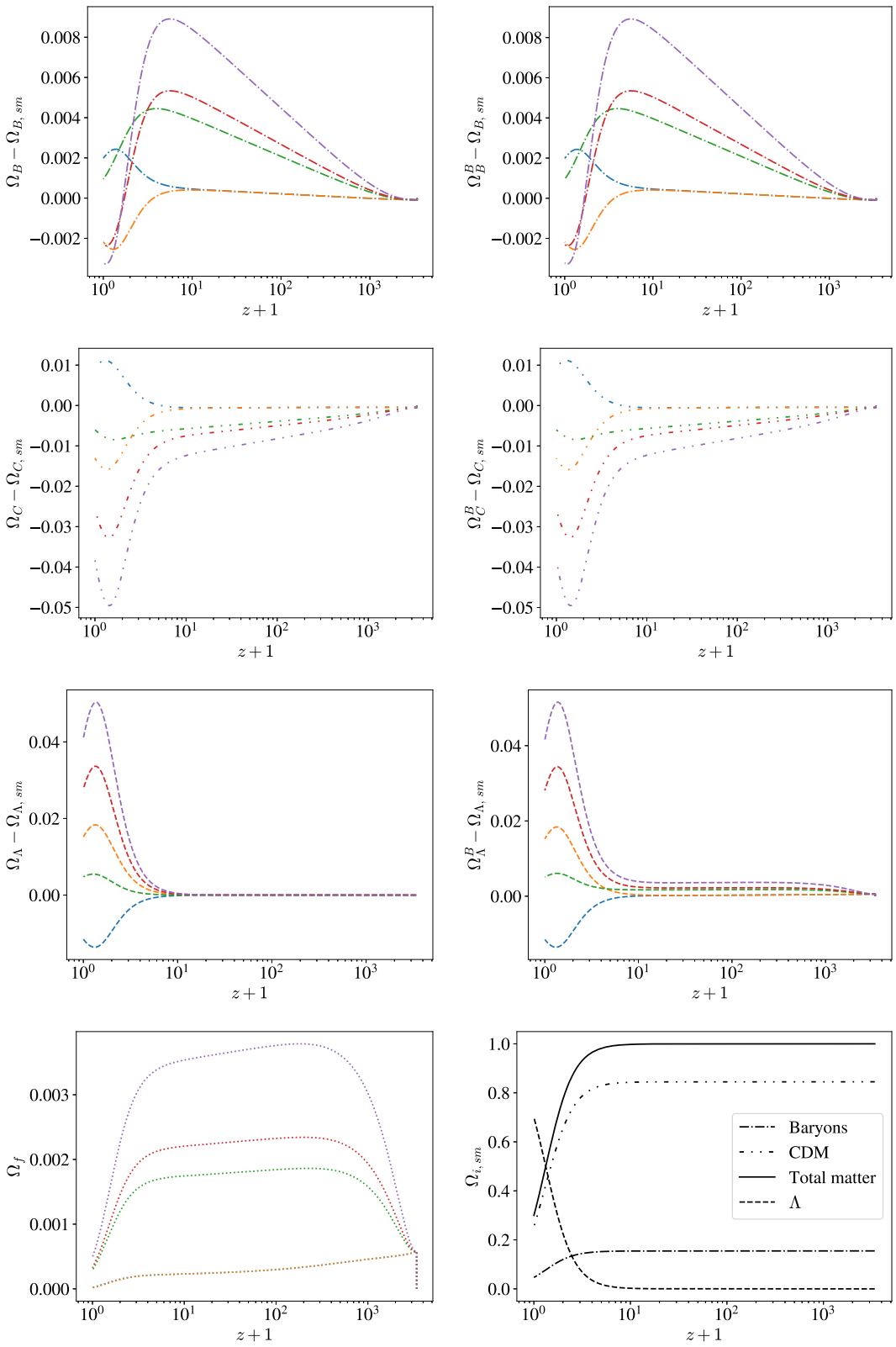

FIG. 5. Evolution of energy contents of the Universe in the Einstein frame (left) and baryon frame (top three figures on the right) as a function of the redshift of the baryon frame. The ΛCDM case is represented in the bottom right figure. Deviations from ΛCDM are represented in the other figures for $\kappa = 10^{-3}$, $\epsilon_B = 10^{-3}$, and values of ϵ_C and $\hat{\rho}_\Lambda$ given in Fig. 3.

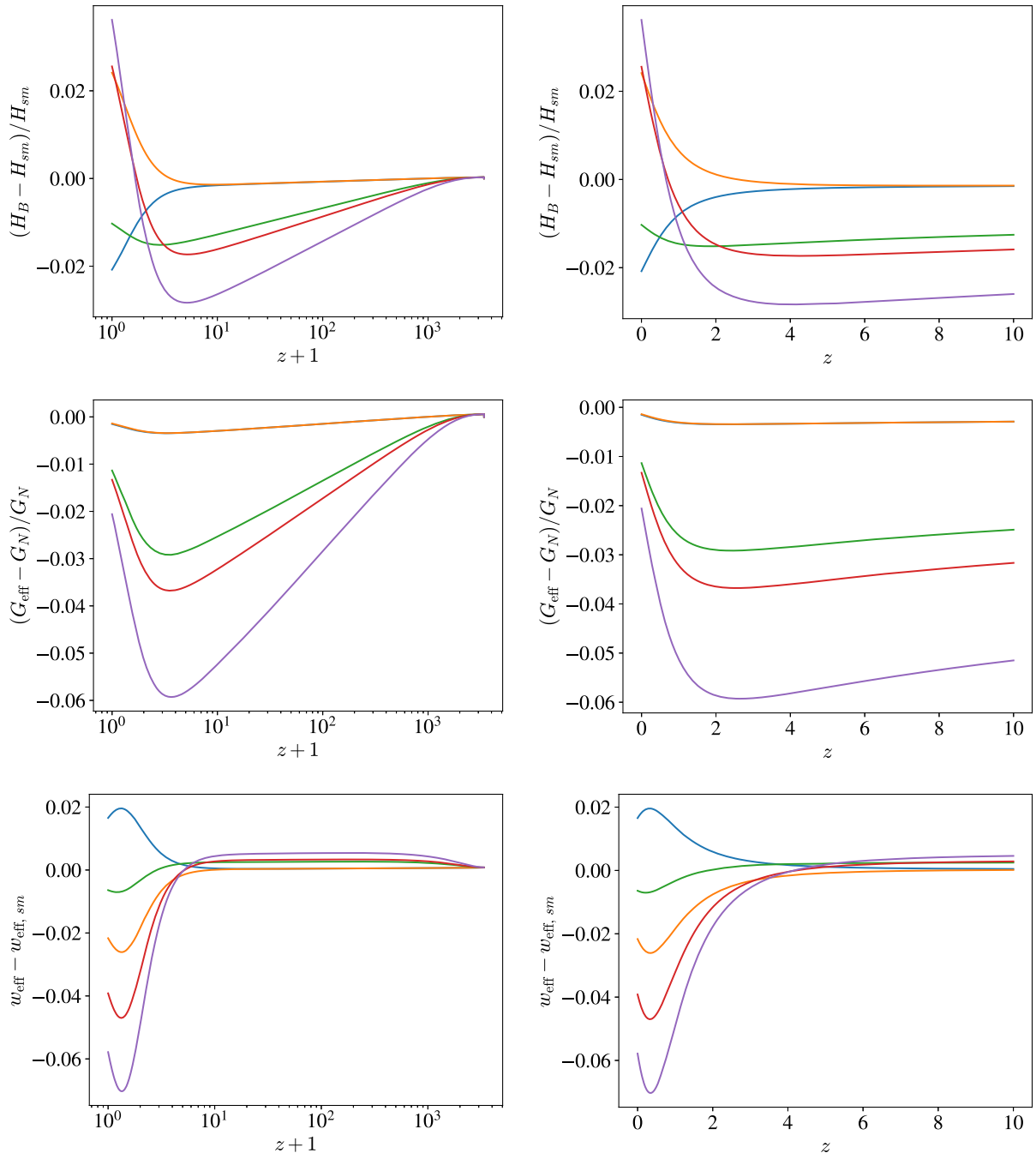

FIG. 6. Evolution of the cosmological quantities H_B, $G_{\rm eff}$, and $w_{\rm eff}$ as a function of the redshift in the baryon frame for $\kappa = 10^{-3}$ and $\epsilon_B = 10^{-3}$. We zoom in on the late evolution on the right. The values of ϵ_C and $\hat{\rho}_\Lambda$ for each color are given in Fig. 3.

initially to a long phase in the matter era where they remain nearly constant before dropping to lower values in the last few e-foldings of the Universe. This has important consequences as the dynamics of the axio-dilaton system and, in particular, the variation of the conformal factors $B_{B,C}$ imply that the matter fractions of the Universe deviate from their ΛCDM values. We also notice that the deviation can be negative by a few percent. This is important as it will hamper the growth of structure and entail a compensation of the extra growth due to the attractive scalar forces by the lower amount of matter in the Universe. This results in a reduced growth of structure in these models.

Figure 6 shows the evolution for the cosmological quantities of interest. In ΛCDM, both $\Delta H_0/H_0$ and $\Delta G/G$ vanish. We observe deviations that become stronger as the parameters move away from the light regions and into the darker ones of Fig. 2. Both also present a maximal negative deviation around $z \sim 2$. At smaller redshifts the

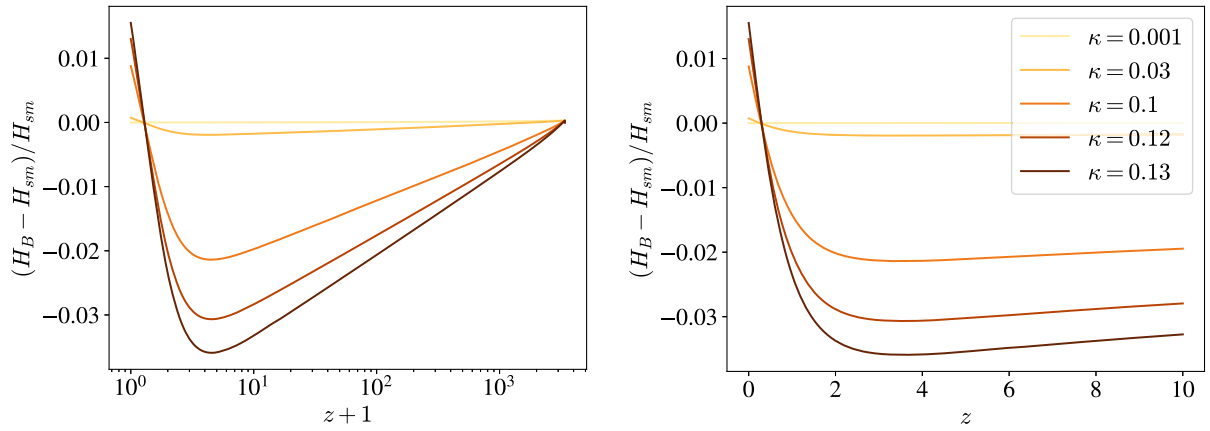

FIG. 7. Deviations of the Hubble rate from ΛCDM for different values of κ, $\epsilon_C = \epsilon_B = 10^{-3}$ and $\hat{\rho}_\Lambda = 7/3$, as a function of the redshift in the baryon frame.

deviation shrinks. This can be attributed to the effect of the cosmological constant which becomes non-negligible at late times. In the case of the red, orange, and purple curves, the deviation crosses 0 and becomes positive. They have in common that their values for the cosmological constant are stronger than the standard model value: $\hat{\rho}_\Lambda \gtrsim 7/3$. Finally, notice that the evolution of $G_{\rm eff}$ shows a negative deviation from Newton's constant in GR. This has two origins which can be traced to its definition (151). First of all, as the effective Newtonian constant is normalized with the Planck normalization for ρ_0, the fact that in Fig. 5 we find that there is less matter in the recent Universe than in ΛCDM implies that $G_{\rm eff}/G_N$ should be less than unity. Another important effect is that the conformal factors $B_{B,C}$ are less than unity too, implying a reduction of $G_{\rm eff}$ compared to G_N. These effects could have been compensated by the extra pull arising from the scalar forces. This is not the case.

Figure 6 also shows $w_{\rm eff}$. It is defined by generalizing (158),

$$w_{\rm eff}(z) := \frac{1}{3}\left(\frac{2q_J(z) - \Omega_{m,0}}{\Omega_{\Lambda,0}} - 1\right). \tag{164}$$

This can simply be seen as a rescaling of the deceleration parameter $q(z)$. In ΛCDM it is easy to see that $w_{\rm eff}$ goes from 0 to -1 (and, equivalently, q from 0.5 to -0.55). Figure 6 shows that for parameters consistent with observations, the deviations are not drastic.

3. Cosmological constraint on κ

We now concentrate on another scenario where the coupling of the dilaton is relaxed from its solar system bound. This is of interest if the dilaton is screened in the solar system and partially on cosmological scales. The largest dilaton coupling allowed by cosmological data is smaller than the supergravity motivated value $\kappa = 1$.

We fix $\epsilon_B = 10^{-3}$, and we look for the highest value of κ such that there are some values of ϵ_C and $\hat{\rho}_\Lambda$ such that the observables are within the observational bounds. We use a precision of the order 10^{-3} relative to the order of magnitude of the parameters. We find that the maximal order of magnitude of κ is 0.1. More precisely, if we also fix ϵ_C and try to find some valid values of $\hat{\rho}_\Lambda$, we find that for $\epsilon_C = 0.1$, $\kappa_{\rm lim} = 0.110$; and for $\epsilon_C = 0.001$, $\kappa_{\rm lim} = 0.124$.

This is illustrated in Fig. 7. Since BAO is the strongest constraint, we look only at the deviations of the Hubble rate in the BAO interval. We can see that for favorable values of the other parameters ($\epsilon_C = \epsilon_B = 10^{-3}$, $\hat{\rho}_\Lambda = 7/3$), κ is allowed at least up to 0.12. However, for $\kappa = 0.13$ the BAO constraint is no longer satisfied. This is of course much less than unity and signals that the dilaton must be cosmologically screened.

V. COSMOLOGICAL PERTURBATIONS

In this section, we study the growth of perturbations for the axio-dilaton models in the matter era in the subhorizon and quasistatic approximation [38]. We obtain the equation governing the evolution of the density contrast $\delta\rho/\rho$ [39].

A. Cosmological perturbations

We focus on small perturbations to the background solutions. We are interested in structure formation, and we evaluate the time evolution of the baryon and CDM density contrasts simultaneously [40]. We only consider the scalar modes of the perturbation of the metric. Using Newton's gauge in the Einstein frame, we have

$$g_{\mu\nu}dx^\mu dx^\nu = R^2(\eta)(-(1+2\Phi_N)d\eta^2 + (1-2\Phi_N)\gamma_{ij}dx^i dx^j) \tag{165}$$

where $\gamma_{ij} = \delta_{ij}$. The cosmological perturbations are defined by

$$\rho_i = \bar{\rho}_i + \delta\rho_i = \bar{\rho}_i(1+\delta_i), \qquad u_i^\mu = \frac{1}{R}(1+\delta v^0, \vec{v}_i) \tag{166}$$

for each field. We also perturb the fields and the axion-matter coupling:

$$\varphi = \bar{\varphi} + \delta\varphi, \tag{167}$$

$$a = \bar{a} + \delta a, \tag{168}$$

$$\mathcal{A} = \bar{\mathcal{A}} + \delta\mathcal{A}. \tag{169}$$

All the symbols with a bar denote background values. The velocity u_i^μ of the two fluids is given by

$$u_i^\mu = \frac{1}{R}(1 - \Phi_N, \vec{v}_i) \tag{170}$$

at linear order. The perturbed Newton's law becomes, for each species,

$$\partial_\eta \vec{v}_i + (\mathcal{H} + \partial_\eta \bar{\chi}_i)\vec{v}_i = -\frac{\vec{\nabla}}{R^2}(\Phi_N + \delta\chi_i). \tag{171}$$

We recognize the scalar force in the Euler's equation due to the interaction with dark matter and the friction term whose origin is the modified Hubble rate $\mathcal{H}_i = \mathcal{H} + \partial_\eta \bar{\chi}_i$ in conformal time and in the Einstein frame.

B. Density contrast of subhorizon modes in the quasistatic regime

We focus on subhorizon modes such that $k \gg \mathcal{H}$, and in the quasistatic regime, $\partial_\eta \sim \mathcal{H}$. Using the Einstein equation

$$\mathcal{R}_{00} - \frac{3}{2\tau^2}(\partial_\eta\tau\partial_\eta\tau + \partial_\eta a \partial_\eta a) - \frac{1}{M_p^2}\left(T_{00} - \frac{1}{2}T g_{00}\right) = 0, \tag{172}$$

and the curvature perturbation

$$\delta\mathcal{R}_{00} = 3\mathcal{H}\Phi_N' + \Delta\Phi_N \approx \Delta\Phi_N, \tag{173}$$

which reduces to the Laplacian of Newton's potential as $3\mathcal{H}\Phi_N' \sim \mathcal{H}^2\Phi_N \ll k^2\Phi_N \sim \Delta\Phi_N$, the Poisson equation then becomes

$$\Delta\Phi_N = \frac{1}{2M_p^2}R^2(\bar{\rho}_B\delta_B + \bar{\rho}_C\delta_C). \tag{174}$$

The perturbed Klein-Gordon equation for φ is

$$\Delta\delta\varphi = -\frac{\kappa}{3M_p^2}R^2(\bar{\rho}_B\delta_B + \bar{\rho}_C\delta_C). \tag{175}$$

Its structure is similar to the Poisson equation. Similarly, we obtain, for the axion field,

$$\Delta\delta a = -\frac{e^{2\bar{\varphi}}}{3M_p^2}R^2(\bar{\rho}_B\epsilon_B\delta_B + \bar{\rho}_C\epsilon_C\delta_C) \tag{176}$$

where we have systematically used the subhorizon and quasistatic approximations. The conservation equation for each species implies that $\rho_i = B_i\rho_{i\text{cons}}$ where the conserved density satisfies

$$\frac{d\rho_{i\text{con}}}{d\tau_i} + 3h_i\rho_{i\text{con}} = 0. \tag{177}$$

In the subhorizon limit, we can identify $\delta_i \simeq \delta_{i\text{cons}}$. This is also the density contrast in the baryon frame as the contributions of both δa and $\delta\phi$ to the change of frame are negligible in the subhorizon limit. This implies that the perturbed conservation equation becomes

$$\delta_i' = -\vec{\nabla}.\vec{v}_i. \tag{178}$$

Now we apply $\vec{\nabla}$ to Eq. (171) and obtain

$$-\delta_i'' - (\mathcal{H} + \bar{\chi}_i')\delta_i' = -\frac{\Delta}{R^2}(\Phi_N + \delta\chi_i). \tag{179}$$

Using the Laplacians from Eqs. (174)–(176), we finally deduce the growth equation for each species in the subhorizon limit,

$$\delta_i'' + (\mathcal{H} + \bar{\chi}_i')\delta_i' - \frac{3}{2}\Omega_B\mathcal{H}^2\left(1 + \frac{\kappa^2 + e^{2\bar{\varphi}}\epsilon_B^2}{3}\right)\delta_B - \frac{3}{2}\Omega_C\mathcal{H}^2\left(1 + \frac{\kappa^2 + e^{2\bar{\varphi}}\epsilon_C^2}{3}\right)\delta_C = 0 \tag{180}$$

in terms of the matter fraction Ω_i in the Einstein frame. We find that the deviations from the standard model have two origins. First, there is the friction term depending on $\mathcal{H}_i = \mathcal{H} + \bar{\chi}_i'$, which is specific to each species as the two fluids couple differently to the axion. Second, there is a modification of Newton's constant for each species on the two effective couplings

$$G_N^i = (1 + 2Q_i^2)G_N \tag{181}$$

such that the perturbation equations become

$$\delta_i'' + (\mathcal{H} + \bar{\chi}_i')\delta_i' - \frac{3}{2}\Omega_B\mathcal{H}^2(1 + 2Q_B^2)\delta_B - \frac{3}{2}\Omega_C\mathcal{H}^2(1 + 2Q_C^2)\delta_C = 0. \tag{182}$$

We have defined the effective couplings

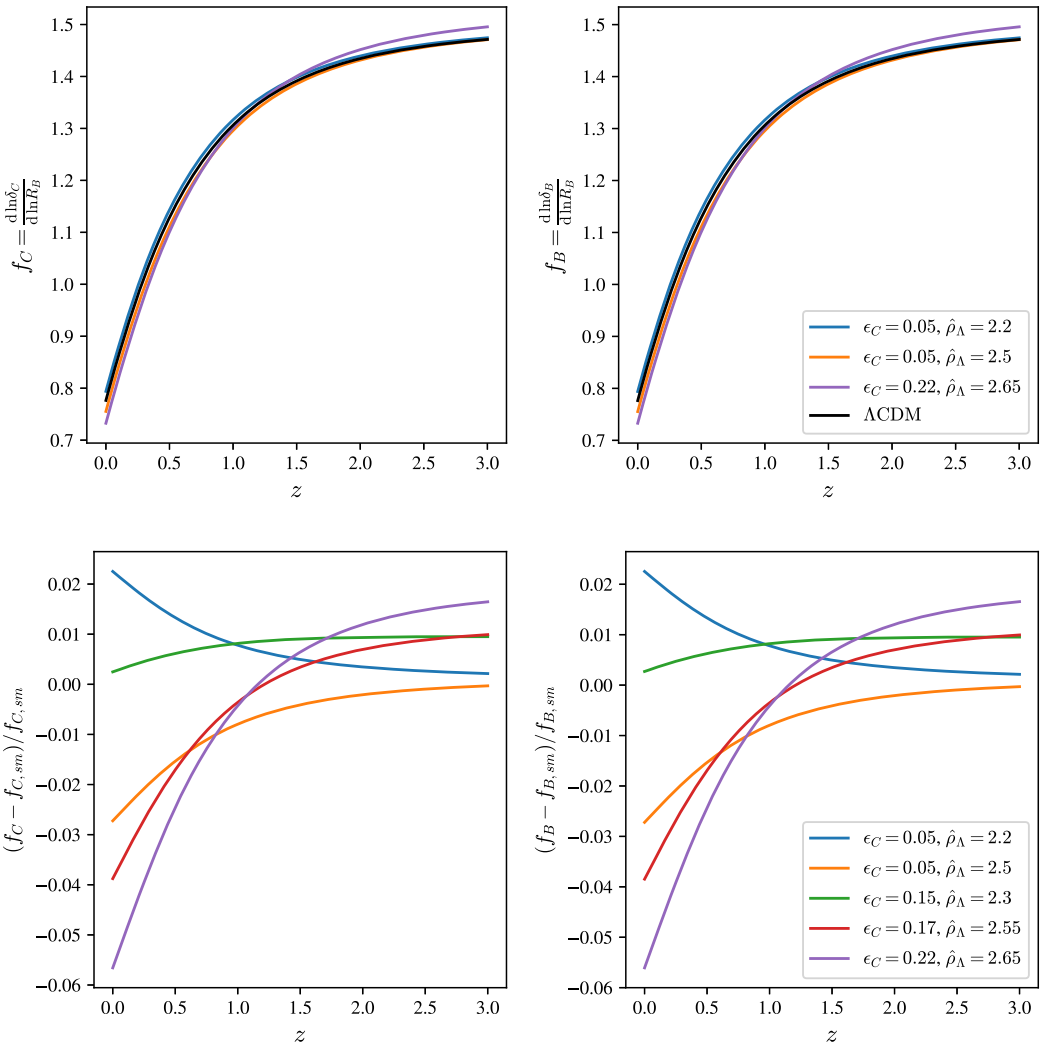

FIG. 8. Growth rate for a few allowed parameters and in ΛCDM, shown for redshifts in the baryon frame $z \leq 3$.

$$Q_i^2 = \frac{\kappa^2 + e^{2\bar{\varphi}}\epsilon_i^2}{6} \tag{183}$$

which parametrize the deviations from ΛCDM. We retrieve that, in the absence of the ϵ_i's, gravity is modified by a factor $\kappa^2/6$ like in the static regime around a compact object. In the following, we solve these equations numerically as a way of investigating the growth of structure for the baryons and CDM.

C. Growth rate

We now focus on the growth rate for small redshifts [41] as defined by

$$f_i = \frac{\mathrm{d}\,\ln\delta_i}{\mathrm{d}\,\ln R_B} \tag{184}$$

where the redshift is deduced from the baryonic scale factor. We represent the growth rates in Figs. 8 and 9. We choose as initial conditions $\delta_i(z_{\rm ini}) \ll 1$ and $\delta_i'(z_{\rm ini})/\delta_i(z_{\rm ini}) \sim \mathcal{H}_{\rm ini}$. We notice that the growth can be either enhanced or disfavored at small redshifts depending on ϵ_C and ρ_Λ. On the other hand, the maximal deviation from ΛCDM is at most five percent. We have also represented the growth factors when κ is varied and both $\epsilon_{B,C}$ are small. Notice that when κ is varied, the growth rate at small redshift becomes smaller and smaller. This is also the case when κ is fixed and ϵ_C is increased. As the effective Newton constants should increase the growth thanks to the presence of fifth forces between particles, we conclude that the background evolution and the effective friction have a drastic effect on the growth of structure. This can be observed in Fig. 5 where the matter density in the late Universe decreases compared to ΛCDM as in [29] where a similar effect was obtained and used to alleviate the σ_8 tension. It would certainly be interesting to see if this trend is also present in the nonlinear regime and could have some consequences for the S_8 tension where less matter clustering is observed at late times than inferred in the ΛCDM scenario [42] from the Planck data

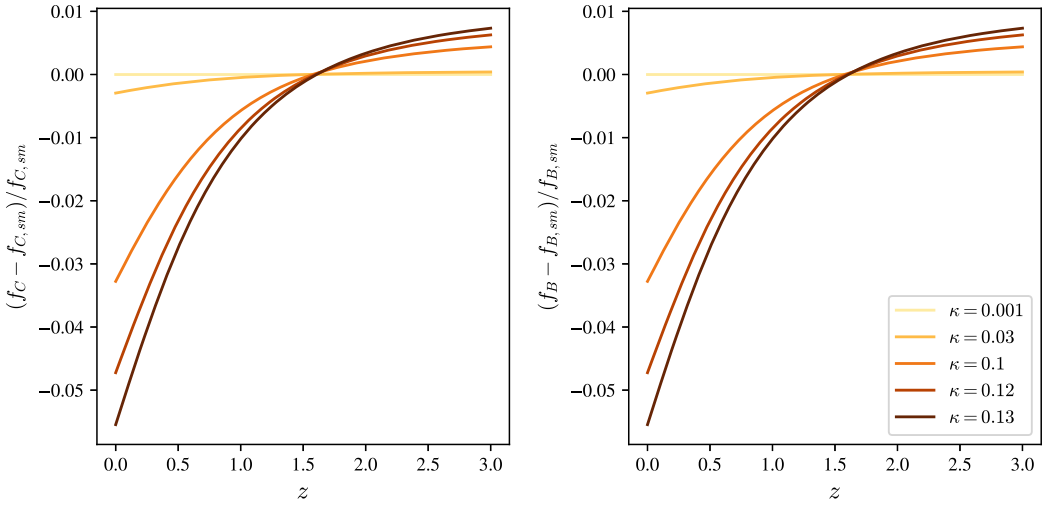

FIG. 9. Growth rate at $z \leq 3$ in the baryon frame for different values of κ and $\epsilon_C = \epsilon_B = 10^{-3}$, $\hat{\rho}_\Lambda = 7/3$.

[3]. The analysis of the S_8 tension in this scenario is left for future work.

Finally, let us remark that we have not taken into account an important effect which would result from both the fact that the effective equation of state w_{eff} (see Fig. 6) is not strictly equal to zero deep into the matter era for $z \gtrsim 2$ and that the perturbations do not behave like in the Einstein–de Sitter universe with $f \neq 1$ (see Fig. 8). This would imply that the Newtonian potential Φ_N in (174) is not strictly constant in the matter era. This could lead to a large integrated Sachs-Wolfe effect (ISW), which is tightly constrained and could appear in the galaxy counts versus the cosmic microwave background cross-correlations [43–45]. This certainly restricts the available parameter space and constrains the possible deviations of the growth factor from ΛCDM. A detailed study of this effect is left for future work.

VI. CONCLUSION

The axio-dilaton model has a clear origin in string theory. We have focused on the screening mechanism introduced in [13] for a constant coupling of the axion to matter, and we have explicitly shown how it can only be effective when the field values at infinity are tuned to specific values. These values should be determined cosmologically. We have studied the background cosmology of these models and shown that the cosmological values do not correspond to the tuned values generically.

In the absence of explicit screening for the axio-dilaton system, which may require one to introduce nonlinear couplings to matter and/or new fields [46] whose dynamics would drive the couplings of the dilaton and the axion to small values in the solar system and larger values cosmologically, we have employed a simple alternative and considered two scenarios. In the first one, the coupling of the dilaton and the axion to baryons is taken to satisfy the solar system constraints and to remain identical to these values on large scales. Only the coupling to cold dark matter is allowed to take much larger values. In this case, we find that the coupling to cold dark matter must be bounded. It turns out that the constraints from BAO at small redshift are the tightest, and the present-day Hubble rate does not deviate from the Planck normalized one by more than three percent. This is not enough to account for the H_0 tension, which lies at the ten-percent level. Similarly, the growth of structure is affected at the five-percent level. Interestingly, in these models growth is not always enhanced, and effectively, a decrease in the growth rate is observed for a large part of the parameter space of the model. This follows from the fact that the growth increase due to the scalar forces is compensated by the decrease of the matter density. This could have some relevance to the σ_8 tension. We hope to come back to this suggestion in the near future. We also consider the case where the axion does not couple significantly to matter and the dilaton couples with a strength κ reduced from the string theory motivated example. We find that κ cannot be allowed values of order unity and must be bounded around 0.1. This entails that the dilaton must not only be screened locally in the solar system but also cosmologically.

Of course, our examples can be modified, and the resulting physics can be very different. For instance, the couplings to matter of both the axion and the dilaton could become nonlinear and therefore lead to screening mechanisms akin to the ones of the symmetron model, for instance. Another possibility would be that other fields could relax to values whereby the couplings of the dilaton and the axion would become very small in the solar system and small cosmologically. The construction of these models is left for future work.

Phenomenologically, the scenarios we have introduced fall within the category of late-time dark energy models where the evolution of the fields at small redshift would

modify both the background cosmology and the growth of structure. As expected, we find that the BAO bound entails a tight constraint on both the possible deviations of the present Hubble rate from its Planck value and the growth factor from its ΛCDM counterpart. We notice that the allowed deviations of the growth factor could reach a few percent and therefore may become detectable by future large scale surveys. The detailed study of the phenomenology of these models is left for future work.

ACKNOWLEDGMENTS

We would like to thank E. Lindner and L. Pogosian for fruitful comments. We would also like to thank A. Ortiz for running some of the long numerical computations. A. O. would like to thank IPhT for funding during his internship, as well as the Physics Department of the Ecole Normale Supérieure for its scholarship.

APPENDIX: VALIDITY OF THE FLAT BACKGROUND APPROXIMATION

We consider that the conditions for the flat background approximation used in Sec. III hold. We assume the exterior solution of Sec. III A and find in which regime the terms neglected by the approximation are indeed negligible. The metric of Sec. III can be written as

$$ds^2 = -(1+2\Phi)dt^2 + (1-2\Psi)(dr^2 + r^2 d\Omega^2). \quad \text{(A1)}$$

The Christoffel symbols, and the Ricci and Einstein tensors for this metric can be found in, e.g., Ref. [47], Sec. 7. The (tt) and (rr) equations from Eq. (13) are

$$\Delta\Phi = \frac{\rho}{2M_p^2}, \quad \text{(A2)}$$

$$(\Delta - \partial_r^2)(\Phi - \Psi) = \frac{3}{4}\frac{(\tau')^2 + (a')^2}{\tau^2}, \quad \text{(A3)}$$

where Δ is the Laplacian. The exterior solution gives

$$\frac{(\tau')^2 + (a')^2}{\tau^2} = \frac{\gamma^2\beta^2}{r^4}. \quad \text{(A4)}$$

Integration then gives us

$$\Phi = -\frac{GM}{r}, \qquad \Psi - \Phi = \frac{3}{16}\frac{\gamma^2\beta^2}{r^2}. \quad \text{(A5)}$$

The deviations from the flat metric are therefore negligible for

$$|\Psi| \ll 1, \qquad \Phi \simeq \Psi. \quad \text{(A6)}$$

This is verified in the regime

$$r \gg GM, \qquad r \gg |\gamma\beta|. \quad \text{(A7)}$$

[1] C. M. Will, Living Rev. Relativity **17**, 1 (2014).
[2] J. L. Feng, Annu. Rev. Astron. Astrophys. **48**, 495 (2010).
[3] N. Aghanim *et al.* (Planck Collaboration), Astron. Astrophys. **641**, A6 (2020); **652**, C4(E) (2021).
[4] E. J. Copeland, M. Sami, and S. Tsujikawa, Int. J. Mod. Phys. D **15**, 1753 (2006).
[5] S. Weinberg, Rev. Mod. Phys. **61**, 1 (1989).
[6] C. de Rham, G. Gabadadze, and A. J. Tolley, Phys. Rev. Lett. **106**, 231101 (2011).
[7] D. Lovelock, J. Math. Phys. (N.Y.) **13**, 874 (1972).
[8] S. Weinberg, Phys. Rev. **138**, B988 (1965).
[9] T. Clifton, P. G. Ferreira, A. Padilla, and C. Skordis, Phys. Rep. **513**, 1 (2012).
[10] T. Damour and G. Esposito-Farese, Classical Quantum Gravity **9**, 2093 (1992).
[11] P. Brax, Rep. Prog. Phys. **81**, 016902 (2017).
[12] T. Damour, F. Piazza, and G. Veneziano, Phys. Rev. Lett. **89**, 081601 (2002).
[13] C. Burgess and F. Quevedo, J. Cosmol. Astropart. Phys. 04 (2022) 007.
[14] C. Vafa, arXiv:hep-th/0509212.
[15] P. Brax, S. Casas, H. Desmond, and B. Elder, Universe **8**, 11 (2021).
[16] A. Avilez and C. Skordis, Phys. Rev. Lett. **113**, 011101 (2014).
[17] B. Bertotti, L. Iess, and P. Tortora, Nature (London) **425**, 374 (2003).
[18] J. Khoury and A. Weltman, Phys. Rev. D **69**, 044026 (2004).
[19] E. Babichev, C. Deffayet, and R. Ziour, Int. J. Mod. Phys. D **18**, 2147 (2009).
[20] A. I. Vainshtein, Phys. Lett. **39B**, 393 (1972).
[21] P. Brax, C. P. Burgess, and F. Quevedo, J. Cosmol. Astropart. Phys. 08 (2023) 011.
[22] O. Lacombe and S. Mukohyama, arXiv:2302.08941.
[23] M. Cicoli, J. P. Conlon, A. Maharana, S. Parameswaran, F. Quevedo, and I. Zavala, arXiv:2303.04819.
[24] S. Alam *et al.* (eBOSS Collaboration), Phys. Rev. D **103**, 083533 (2021).
[25] L. Amendola, Phys. Rev. D **62**, 043511 (2000).
[26] L. Amendola, T. Barreiro, and N. J. Nunes, Phys. Rev. D **90**, 083508 (2014).
[27] L. Verde, T. Treu, and A. G. Riess, Nat. Astron. **3**, 891 (2019).
[28] E. D. Valentino, O. Mena, S. Pan, L. Visinelli, W. Yang, A. Melchiorri, D. F. Mota, A. G. Riess, and J. Silk, Classical Quantum Gravity **38**, 153001 (2021).

[29] B. J. Barros, L. Amendola, T. Barreiro, and N. J. Nunes, J. Cosmol. Astropart. Phys. 01 (2019) 007.
[30] E. Di Valentino *et al.*, Astropart. Phys. **131**, 102604 (2021).
[31] R. C. Nunes and S. Vagnozzi, Mon. Not. R. Astron. Soc. **505**, 5427 (2021).
[32] L. Amendola *et al.*, Living Rev. Relativity **21**, 2 (2018).
[33] F. S. Accetta, L. M. Krauss, and P. Romanelli, Phys. Lett. B **248**, 146 (1990).
[34] J.-P. Uzan, Rev. Mod. Phys. **75**, 403 (2003).
[35] U. Seljak *et al.*, Phys. Rev. D **71**, 103515 (2005).
[36] P. Peter and J.-P. Uzan, *Primordial Cosmology* (Oxford University Press, Oxford, United Kingdom, 2005).
[37] E. V. Linder, arXiv:2304.04803.
[38] L. Pogosian and A. Silvestri, Phys. Rev. D **94**, 104014 (2016).
[39] G.-B. Zhao, L. Pogosian, A. Silvestri, and J. Zylberberg, Phys. Rev. D **79**, 083513 (2009).
[40] D. Huterer *et al.*, Astropart. Phys. **63**, 23 (2015).
[41] DESI Collaboration, arXiv:1611.00036.
[42] V. Poulin, J. L. Bernal, E. Kovetz, and M. Kamionkowski, Phys. Rev. D **107**, 123538 (2023).
[43] R. G. Crittenden and N. Turok, Phys. Rev. Lett. **76**, 575 (1996).
[44] S. Khosravi, A. Mollazadeh, and S. Baghram, J. Cosmol. Astropart. Phys. 09 (2016) 003.
[45] G. Benevento, N. Bartolo, and M. Liguori, J. Phys. Conf. Ser. **956**, 012001 (2018).
[46] C. P. Burgess, D. Dineen, and F. Quevedo, J. Cosmol. Astropart. Phys. 03 (2022) 064.
[47] S. Carroll, *Spacetime and Geometry* (Addison Wesley, Reading, MA, 2004).